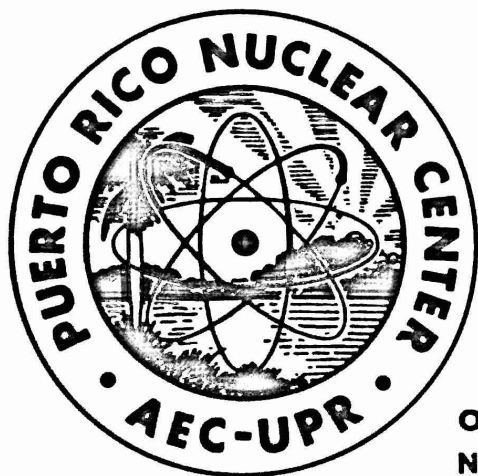PRNC-128

PUERTO RICO NUCLEAR CENTER

MATRIX ISOLATION STUDIES OF THE GAMMA
RADIOLYSIS OF HETEROCYCLIC MOLECULES

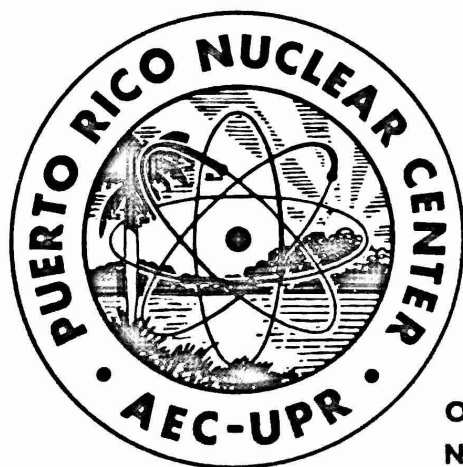Progress Report 4

April 1969

PUERTO RICO NUCLEAR CENTER

MATRIX ISOLATION STUDIES OF THE GAMMA RADIOLYSIS OF HETEROCYCLIC MOLECULES

Progress Report 4

A. Grimison and G. A. Simpson

April 1969

TABLE OF CONTENTS

Page

PERSONNEL PARTICIPATING

Dr. A. Grimison, Chief Scientist, Principal Investigator

Dr. G. A. Simpson, Associate Scientist

M. Trujillo Sánchez, Graduate Student Assistant

F. Bernasconi, Graduate Student Assistant

O. Pérez, Research Assistant (Part time)

The results achieved in this project from May 1966 to April 1968 were previously presented in Technical Progress Reports No. 1 (PRNC No. 88), No. 2 (PRNC No. 99) and No. 3 (PRNC No. 116). The present Technical Progress Report reviews the results obtained in the period from April 1968 to April 1969, the time of preparing this Report. As has been done previously, the report is divided into two sections, Experimental and Theoretical.

Section A. Experimental Results

I. General Procedures

Purification of solvents, such as 2-methyltetrahydrofuran (MTHF) or 3-methylpentane (3MP) have been described previously.[1a,b,c] All compounds used were of highest commercial purity. Absorption spectra were obtained as before.

Visual observations of either high or low temperature irradiated compounds were made in a darkened room after suitably dark adapting the observers eye. Quantitative measurements of relative thermoluminescent intensities were obtained with a commercial instrument, the Con Rad Thermoluminescent detector, under nitrogen purging to minimize combustion. No evidence of combustion was found. The device is calibrated in terms of rad-equivalents of LiF thermoluminescence. Thus, absolute comparison are possible.

ESR measurements were performed both with the Varian 4500 at IVIC, Venezuela, and with the Varian E-3 of the Chemistry Department, U.P.R. Estimations of "spin" concentration were made in terms of the rated instrument sensitivity 10^{11} spins/gauss.

A description of the experimental conditions for observing luminescence effects is found in Figures 3, 4 and 5 along with detailed list of components in Table 2. A discussion of their applications can be found in the Section "Photoionization of Heterocyclics at 77°K".

II. Absorption Spectra of Radiolytic Intermediates at 77°K

A copy of a paper submitted to the Journal of Physical Chemistry is found in Appendix 1. This paper, entitled "Electron Attachment by Pyridine and the Diazines in Gamma-Radiolysis at 77°K", represents a finalization of studies revealed in previous Technical Progress Reports.

Electron attachment in these compounds has been observed following gamma radiolysis in MTFH glassy solutions. This observation has been confirmed by studies of bleaching effects, solvent concentration effects and through competition effects with added electron scavengers. The experimental spectra of anions are in excellent agreement with spectra obtained by classical chemical procedures.

III. Thermoluminescence Following Gamma-Radiolysis at 77°K

Thermoluminescence of irradiated biologically significant compounds on warming from 77°K has been reported previously.[2,3,4] Lehman and Wallace[2] have made extensive quantitative studies on a large number of compounds. Among them are adenine, having a thermoluminescence maxima at 480 nm, cytosine, DNA, guanine (maxima at 510 nm), thymine and uracil. Approximate estimations of the G values for thermoluminescence can be made from their data and are of the order 10^{-1} photons per 100eV absorbed for adenine, the most efficient and for uracil, 10^{-4} photons/100 eV. This technique

is very sensitive, with a minimum thermoluminescence yield on the order 10^{-7} photons/100 eV detected. Fleming and Kerr[3] have observed thermo-luminescence from adenine and cytosine with maxima near 480 nm, and which was identical to the crystal phosphorescence under uv excitation. Charlesby and Singh[4] have likewise reported identifal uv induced blue phosphorescence and thermoluminescent bands of irradiated purine and pyrimidine bases. Thus, our visual observations of blue thermoluminescence from those compounds reported in Table 1 are in agreement both in relative magnitude and in wavelength region with the previous studies.

Studies of the phosphorescence of these compounds in aqueous solutions would place the emission bands of those compounds in the violet rather than the blue regions of the spectra. For example, Longworth, Rahn, Schulman[5] have reported that adenine has phosphorescence bands occuring between 365 and 425 nm, and guanine at 400 nm in neutral water. Nevertheless, the fact remains that uv excitation of the crystals produce blue emissions.[2,3,4] Thus it may be concluded that the entities in neutral water are strongly aquated. Shifts of 50 nm may well be ascribed to strongly perturbed N-II transitions, and can be observed in aqueous solu-tions.

IV. Thermoluminescence and ESR Signals after Room Temperature
    Gamma-Radiolysis

Production of long lived free radicals in the crystalline purine of pyrimidine bases by ionizing radiation has been observed previously. The works of Andros and Calvin,[6] or Cook and Elliot[7] provide good reference. Similarly, for those compounds irradiated at 77°K, literature

exists for comparative studies of both ESR and thermoluminescence of irradiated bases, viz. Sonner and Pihl.[8] However comparative ESR and thermoluminescence studies for those compounds irradiated at room temperature have not been made. Presumeably, the existence of a high temperature thermoluminescence has not been observed.

In figures 1 and 2 we report the ESR spectra of irradiated cytosine and uracil. The G values for production of those radicals are estimated to be of the order 10^{-4} and 10^{-3} spins/100 eV respectively. The radicals associated with these unsymmetrical and unresolved spectra have g values of 2.02 and widths at half maximum intensity of less than 20 gauss. The absence of detail is characteristic of powdered samples. The g values, width and absence of large splittings suggest the presence of neutral radicals having an unpaired electrons localized on a carbon atom joined to at least one hydrogen atom. The similarity in the spectra of the cytosine and uracil radicals allow the suggestion that a hydrogen may have added to the carbon atoms at the 4 or 5 position in the ring. This interpretation is at least consistant with the single crystal study of Cook and Elliot,[7] where the presence of a radical of cytosine with an extra H atom in the 5 position in addition to a radical with an H atom vacancy from the nitrogen in the 3 position is reported.

In addition, the ESR spectra are sensitive to moderate heating following gamma irradiation. Heating samples of irradiated cytosine or uracil to 50°C causes a reduction in the intensity of the ESR spectra.

High temperature thermoluminescence from purine or pyrimidine bases has been observed in these laboratories. The following compounds and their

relative intensities of thermoluminescence were obtained with a commercial thermoluminescence detector after irradiating to a dose of 3.5×10^5 rads:

Cytosine	16.	Thymine	1.3
Adenine	15	Purine	0.6
Uracil	9.1	Guanine	0.1

LiF - 10^4

All of the thermoluminescent intensities were linear in dose up to the value noted. Further, the visual observation of the temperature dependence of the luminescence places the maximum glow intensities in the range 64°C to 155°C (which were limits of temperatures at which feeble glows could be observed).

Work is anticipated to determine the quantitative aspects of the temperature dependence of both the free radical concentration and the thermoluminescence process. A tentative hypothesis, which we wish to test, is that the destruction of the free radical centers gives rise to the thermoluminescence, that it may be chemiluminescence. This process is distinct from that responsible for the luminescence reported in part III, which we suspect to be due primarily to recombination of an electron-cation pair which has stability at 77°K.

(The assistance in experimental work of Dr. H. Bemski, IVIC, Venezuela is gratefully acknowledge).

V. Photoionization of Heterocyclics at 77°K

A survey of the pertinent literature indicates the existence

of some four mechanisms whereby a neutral atom or molecule may be liberated from a velance electron. These are:

1. Direct photoionization

2. Charge transfer to the solvent (CTTS)

3. Biphotonic photoionization

4. Lim proposal

The first mechanism is, perhaps, the most well known of the four and is the process responsible for the production of the ionisphere. On absorption of a photon having energies greater than or equal to the ionization potential of the compound a cation and a separated electron are produced. Presumeably, this process can also occur in condensed phases, but the photon energy required may be lowered due to the solvation energies of the resultant ions. Since there is a one to one correspondence between photons absorbed and ions produced the rate law for the overall process is linear with respect to intensity of the exciting light.

The second mechanism is suitable for the effect of light absorption by ions in highly polar solvents such as water. It differs from the first in that it applies to a specfic solution electronic transition - charge transfer absorption bands - and is highly influenced by temperature, solvent dielectric and the presence of added salts. It is also a one photon process and can be characterized by the equation.

$$(ion) + h\nu \longrightarrow (ion)* \longrightarrow (ion)^{-1} + e^{-}_{solvated}$$
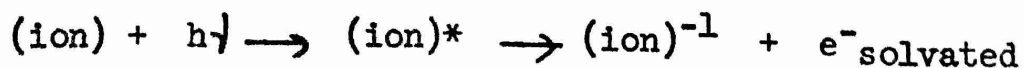
This mechanism is known to occur for the halide ions, ferric salts and some neutral species.[9]

The third process may well be the most important for biological entities. It can provide a low energy route towards photobiological damage, energy storage, or conversion in biological systems. The mechanism has been demonstrated to occur in aromatic amines by Albrecht,[10] and in aromatics by Porter.[11] The mechanism requires that a long lived triplet state, initially produced by light absorption by a neutral, absorb a second photon to produce the electron-cation pair. Generally the photon energy required is less than half that of the gaseous ionization potential. Since two photons are required the rate is a function of the square of the light intensity.

The final mechanism, a one photon ionization of the negative acridine dye ions has been proposed by Lim. The mechanism has many features in common with the CTTS mechanism and requires further experimental work to substantiate its uniqueness.

Thus, the problem in demonstrating the occurrence of photo-ionization among heterocyclics becomes one of determining the appropriate mechanism of the process. In Progress Report No. 116[1C] we have demonstrated that some compounds on exposure to ultraviolet light at 77°K produced colored intermediates. We suggested that photoionization occurs in those cases. However, the procedures used were unsatisfactory in producing measurable amounts of absorbances. Thus, it was decided to use an altogether different approach, luminescence detection, which would be inherently more sensitive than an optical

absorption technique. Therefore, we will present our investigations
of the luminescence behavior of indole, indazole, purine and tetra-
phenylpyrrole (triphenylamine and aniline were used as referents). The
tests we employ are designed to demonstrate the occurrence of recombina-
tion luminescence, whether it is produced in the forms of prolonged
isothermal luminescence, infrared stimulated luminescence, or thermo-
luminescence. The time dependence of isothermal prolonged luminescence
was described by Debye and Edwards[13] as having an intensity-time rela-
tion of the form $I = k_t{}^{-M}$, were k is a constant and proportional to
the total integrated prolonged luminescence; t is time after cessation
of exciting light, and M, a number having an unknown dependence on
concentration, being very close to unity for very low concentrations
of test compound and decreasing with increasing concentration. This
time dependence results from the diffusion controlled migration follow-
ing thermal excitation of trapped electrons in the fields of cationic
centers in rigid media at reduced temperatues. Skelly and Hamill[14]
have shown that absorption of infrared light into the trapped electron
absorption band causes migration of trapped electrons resulting in
stimulated luminescence on recombination with a neighboring trapped
cation. Finally, Daniels[15] has shown that thermal stimulation by
increasing temperatures causes recombination luminescence in the form
of thermoluminescence. Typically the luminescence observed under all
of these conditions is the phosphorescence of the neutral compound.

The experimental arrangement consisted of an intense uv light
source, with appropriate filters for isolating the excitation

wavelength, a light tight housing for the optical dewar and cell, and a high intensity grating monochromator, along with photomultipliers, power supply, electrometer and recorders. The actual arrangements are found in Figures 3, 4, and 5, with a legend of the components in Table 2. In Figure 3, the arrangement used in obtaining normal phosphorescence, fluorescence or prolonged luminescence spectra is described. Figure 4 shows the arrangement used in obtaining emissions under infrared stimulation. Finally in Figure 5 is shown the arrangement used to measure total luminescence during isothermal, infrared, or warm up stimulation of the photolyzed glassy solutions.

A demonstration of the resolution achieved by this apparatus can be found in Figure 6 where the emission spectra of benzene produced by 250 mm excitation in 3MP at 77°K is demonstrated. Comparison with data given in Pringshem[16] shows the position of the maxima to be correct to within ± 0.8 mm with a resolution of 10 mm. Higher resolution is possible. The reference curve shown below the benzene emission was obtained with pure 3MP and demonstrates the absence of contaminating impurities, scattered light or dewar emission. The lifetime of benzene phosphorescence was also determined as a test by shutting off the light source rapidly or flashing the General Radio Co. stroboscope and monitoring the decay on a recorder or oscilloscope. This result can be found in Figure 7. The lifetime obtained 4.7 ± 0.3 sec is in good agreement with some recent work of Kalantar.[17]

As a further test of technique, the lifetime of the stroboscope flash was determined. The result of this test is found in Figure 8.

The half intensity durations, and the decay times are measured as: low intensity, 2.7 μ sec. duration and 1.8 μ sec decay; med. intensity, 3.0 μ sec. duration and 2.1 μ sec decay; and high intensity, 5.3 μ sec. duration and 3.1 μ sec decay. The relative intensities of the three levels shown in Figure 8 are proportional to the actual lamp intensities. The manufacturer quotes the duration as approximately 2 seconds shorter than those obtained here. This indicates that some undesired capacitances are present in our detection circuit. The presence of departures from linearity in the decay plot is consistant with this. Thus, emission lifetimes can be measured to some 10's of μ sec with good accuracy.

The results of the luminescence measurements on indole, indazole, purine, tetraphenylpyrrole, aniline or triphenylamine in MTHF at 77°K can be characterized by Figures such as No. 9 through 13. In general, if any of those compound are exposed to the full output of a high pressure mercury arc for times as low as 1 second, the decay of luminescences show a time dependence similar to that found for indole in Figure 9. The overall time dependence can be expressed by the equation $I = A_{exp}-(t/\gamma) + B\, t^{-M}$. The departure of the curve in Figure 9 at early times is a result of plotting the $\exp-(t/\gamma)$ function on a log-log scale. Equations for the six compounds have been found for 5 second exposures and are expressed as:
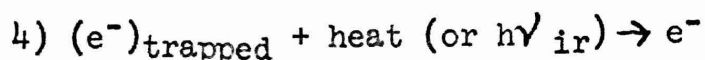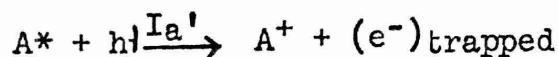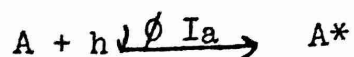
Compound		Function

Aniline $\qquad$ $I = 3.0 \times 10^{-2} \exp{-(t/4.8 \pm 0.3 \text{ sec})}$

$+ 3.8 \times 10^{-4} \ t{-}1.02 \text{ amp.}$

Indole $\qquad$ $I = 1.9 \times 10^{-2} \exp{-(t/6.4 \pm 0.2 \text{ sec})}$

$+ 1.7 \times 10^{-5} \ t^{-0.93}$

Indazole $\qquad$ $I = 6.0 \times 10^{-2} \exp{-(t/3.5 \pm 0.1)}$

$+ 3.6 \times 10^{-6} \ t^{-0.94}$

Triphenylamine $\qquad$ $I = 1.6 \times 10^{-4} \exp{-(t/4.8 + 0.3 \text{ sec})}$

$+ 5.0 \times 10^{-6} \ t^{-0.83}$

Purine $\qquad$ $I = 5.0 \times 10^{-2} \exp{-(t/1.6 + 0.1 \text{ sec})}$

$+ 2.8 \times 10^{-7} \ t^{-0.86}$

Tetraphenylpyrrole $\qquad$ $I = 6.3 \times 10^{-3} \exp{-(t/1.6 \pm 0.1 \text{ sec})}$

$+ 2.5 \times 10^{-6} \ t^{-0.92}$

The concentrations of all compounds are of the order 10^{-4} in MTHF.
The rapidly decaying portion of the mathematical function is the
normal first order decay function, and the values of Υ obtained here
agree well with the literature values where available. The prolonged
luminescence is described well by the Debye-Edwards function. There
is no departure from this function for a time range from 90 seconds
to at most 3 hours later when the photo multiplier dark current is
reached. There is a good correlation between the magnitude of the
phosphorescence decay constants and the magnitude of the Debye-
Edwards proportionality constant. That is, the greater the lifetime,
the greater the prolonged luminescence. This suggest the involvement
of the triplet state in the photoionization of these compounds.

In figure 10 is found the emission spectra obtained during a period from 90 seconds to six minutes after the cessation of the exciting light for indole, indazole and aniline(with a 40 mm band pass). The spectrum obtained for indole agrees with that obtain by Freed and Slamre,[18] and that of aniline with the spectrum of Lewis and Kasha[19]. Thus, as pointed out earlier, the phosphorescent state of the neutral is produced by recombination.

The effect of infrared stimulation on the prolonged luminescence of a 2×10^{-3}M solution of aniline is found in Figure 11. The effect of infrared stimulation is to change the value of the Debye-Edwards exponent from 0.8 to 1.6. This observation is consistant with effects noted by Skelly and Hamill.[14] We also observe an increase in the Debye-Edwards exponent during ir stimulation of indole and indazole solutions.

The dependence of the total recombination luminescence on the intensity of exciting light is shown in Figures 12 and 13 for aniline and indole as the ratio of the square of the total exciting light intensity I ex divided by the integrated luminescence Σ. If a biphotonic photoionization involving the triplet state occurs, then the process can be described by the following mechanism.

$$A + h\nu \xrightarrow{\phi \ I_a} A*$$

1) $A* \longrightarrow A + h\nu'$

2) $A* \longrightarrow A$

$$A* + h\nu \xrightarrow{I_a'} A^+ + (e^-)_{trapped}$$

3) $A^+ + e^- \longrightarrow A*$

4) $(e^-)_{trapped} + heat \ (or \ h\nu_{ir}) \rightarrow e^-$

A represents a neutral compound, A* its excited triplet state, and A^+ is its cation. ϕ represents the quantum yield of intersystem crossing and the product of ϕ and I_a, the light absorbed by the neutral, is the rate of populating the triplet state. I_a' is the intensity absorbed by the triplet state. The trapped electron is indicated by $(e^-)_{tr}$ and e^- is a free electron.

These equations can be solved by the steady state approximation if we assume that the overall rate of repopulating the triplet state, by steps 3 and 4 are very much slower than the rates of formation. This is a justifiable approximation, since we observe that a one second exposure to the exciting light produces cation and electron pairs that require two to three hours to recombine. The particular solution we present here requires weak absorption - which we can control by concentrations, and ideally narrow wavelength band absorptions. Narrow band absorptions were not possible, so that extinction coefficients referred to are the average over the absorption bands. The solution is

$$= \frac{I_o{}^2 \; \emptyset \, \epsilon \, e' \, \gamma \, A \quad d}{1 + I_o \; \epsilon' \, \gamma \; d} \; \Delta \, T.$$

Σ refers to the total number of ionization events produced during the excitation period ΔT, Io is the incident exciting light intensity; ϵ, and ϵ' refer to the extinction coefficients of the neutral and triplet state respectively, d the optical path length; i.e. 1 cm, and γ is the natural lifetime of the triplet or $= 1/(k_1 + k_2)$. Thus, the relationship requires that $I_o{}^2/\Sigma$ have a linear dependence on the exciting light intensity.

We take the value of the quantity Σ, to be proportional to either the total amount of prolonged luminescence, the total amount of infrared stimulated luminescence, or the total amount of thermo-luminescence. This quantity, measured Coulombs of photomultiplier current, is plotted in Figures 12 and 13, according to the above expression and the data is obtained from the three forms of recombination luminescence. The ratio $I_o{}^2/\Sigma$ is linear with I_o, but is plotted on a semilog scale for convenience.

The data referred to as electrical integration was an attempt to accumulate the photomultiplier current on a capacitor, in contrast to a manual method of integrating the photomultiplier current vs. time -from a strip chart recordings - by a graphical method. The Σ acquired in this fashion is very much lower than from the other methods. This is not to be taken as evidence that considerably less recombination occurs during warming but rather that the capacitor used in the measurement

lost a considerable fraction of its accumulated charge through leakage during the course of the experiment. Comparative data for the Σ obtained during warming showed that the electrical method gave data lower by two orders of magnitude than the manual integration method. In Figure 12, the isothermal and infrared stimulation data were performed with a concentration of 2×10^{-4}M aniline, while the thermoluminescencent data for aniline were obtained with a concentration of the order 10^{-3}M. The data presented in Figure 13 were obtained with an indole concentration of 5×10^{-4}M.

The existence of the Debye-Edwards intensity dependence, the effects of infrared stimulation, and the thermoluminescence indicate the occurrence of photoionization among these compounds. The existence of a squared intensity dependence in agreement with a biphotonic mechanism involving the triplet state, indicates the path by which photoionization has occurred in the cases of indole, indazole and aniline. The occurrence of biphotonic photoionization in aniline has been observed previously.[10, 11]

Section B: Theoretical work

The theoretical work has continued along the basic lines indicated previously. One objective of this part of the program is the calculation of excitation energies of radical anions and cations of heterocyclic molecules, to aid the assignment of experimental spectra. The other objectives include the general features of the electronic structure of such species, and work has also been begun on electron-molecule interactions.

I. Electronic Spectra of Heterocyclic Radical Cations and Anions

The results which have been obtained for the doublet-doublet transitions of the radical anions of pyridine, pyrimidine, pyrazine and pyridazine are fully described in the appended article, which has been submitted for publication. These calculations use the Pariser-Parr-Pople self-consistent field method, with and without Configuration Interaction. The results can be summarized by saying that an excellent agreement was obtained with experimental and theoretical results of other groups of workers,[20,21] as well as with the experimental work reported earlier. The use of limited Configuration Interaction does not improve the agreement with experiment, in harmony with recent theories.[22]

In addition to the above calculations, the radical cations of the following molecules were examined: pyrrole, furan, thiophene, pyridine, pyrimidine, pyrazine, and pyridazine. A very much poorer agreement with experiment is obtained for the radical cations. The Pariser-Parr-Pople method uses the pi-electron approximation, so that these results question its validity for such radical cations. For the anions the unpaired electron is certainly in an antibonding pi-orbital, and the approximation appears to give good results. However, for the radical cations of heterocyclic molecules, it is by no means certain whether an electron has been removed from a sigma (non-bonding) or from a pi-orbital. Pyrrole is the only cation which has been examined which has no non-bonding electrons available, but

the results for the pyrrole cation are equally bad. This indicates
that as well as taking account of the sigma-electrons, it may be necessary
to specifically include the sigma-pi interaction terms. These give rise
to a reorganization in the sigma-framework on ionization of a pi-electron,
which will significantly affect the stability of the radical cation.[23-25]
This point is currently being investigated. No method exists at present,
apart from al initio calculations, which includes this type of interaction.

II. Valence-Bond Calculations on Heterocyclic Systems

These calculations use cyclopentadiene as a preliminary model,
and aim at the electronic structure of simple heterocyclic molecules and
radicals, using a non-empirical valence bond method, as described in
previous Reports. During this year, work has been principally on the
modification of a program originally written by Dr. Palmieri (University
of Bologna). This uses as input the atomic integrals whose calculation
was described in Technical Progress Report No. 3 (PRNC-116). All possible
determinantal basis functions of a given multiplicity are generated,
and the integrals among them evaluated using Lowdin's density matrix
formation for non-orthogonal Slater determinants.

III. Hetaryne Intermediates

In collaboration with Dr. W. Adam (U. of Puerto Rico) and
Dr. R. Hoffmann (Cornell U.) a study has been completed of the 'hetaryne
intermediates' formed by removal of hydrogen atom(s) from heterocyclic
molecules. This work has been accepted for publication, and a copy
is appended to this Report. The electronic structure of these

intermediates was examined by the Extended Huckel Theory,[26] which includes sigma- and pi-valence electrons. The trends in stability correlate very well with experimental data, and were analyzed in terms of orbital splitting patterns.

IV. Electron-Molecule Interactions

Work is beginning on the calculation of exact molecular potentials between an electron and a many-electron molecule, in the form of a multipole expansion.[27] This potential is to be used in investigations of electron-molecule attachment processes.

BIBLIOGRAPHY

1. a) A. Grimison, Technical Progress Report No. 1, PRNC No. 88.

    b) A. Grimison, Technical Progress Report No. 2, PRNC No. 99.

    c) A. Grimison, and G. A. Simpson, Technical Progress Report No. 43, PRNC No. 116.

2. R. L. Lehman and R. Wallace, p. 43, "Electronic Aspects of Biochemistry," Academic Press, N.Y., (1964).

3. R. J. Fleming and R. M. Kerr, Nature 206, 119 (1965).

4. B. B. Singh and A. Charlesby, Photochem. and Photobiology, 5, 63 (1966).

5. J. W. Longworth, R. O. Rahn and R. G. Schulman, J. Phys. Chem. 45, 2930 (1966).

6. G. M. Andros, and M. Calvin, Biophysical Jour, 2, 217 Suppl. (1963).

7. J. B. Cook, J. P. Elliot and S. J. Wyard, Mol. Phys. 13, 49 (1967).

8. T. Sooner and A. Pihl., Acta Chem. Scand. 20, 266 (1966).

9. G. Stein, p. 230, "The Solvated Electron", Advances in Chemistry No. 50, Washington, D.C. (1965).

10. K. D. Cadogan and A. C. Albrecht, J. Phys. Chem. 72, 929 (1968).

11. W. A. Gibbon, G. Porter, and M. I. Savadatti, Nature 206, 1355 (1965).

12. E. C. Lim, C. P. Lazzarro and G. W. Swenson, J. Chem. Phys. 43, 970 (1965).

13. P. Debye and J. O. Edwards, J. Chem. Phys. 20, 236 (1952).

14. D. W. Skelly and W. H. Hamill, J. Chem. Phys. 43, 3497 (1965).

15. F. Daniels, D. F. Saunders, "Thermoluminescence of Crystals, Final Report", University of Wisconsin (1951).

16. P. Pringsheim, "Fluorescence and Phosphorescence", Interscience, N.Y., (1961).

17. T. E. Martin and A. H. Kalantar, J. Phys. Chem. 72, 2265 (1968).

18. S. Freed and W. Salmre, Science 128, 1341 (1958).

19. G. N. Lewis, and M. Kasha, J. Am. Chem. Soc. 66, 2100 (1944).

20. J. W. Dodd, F. J. Hopton, and W. S. Hush, Proc. Chem. Soc. (London) 61 (1962).

21. P. I. Kimmel and H. L. Strauss, Abstract of Papers, American Chemical Society Meeting, San Francisco, March 31, 1968 S-151, and private communication from H. L. Strauss.

22. N. L. Allinger and T. W. Stuart, J. Chem. Phys., 47, 4611 (1967).

23. T. H. Dunning and V. McKoy, J. Chem. Phys., 47, 1735 (1967).

24. J. M. Schulman and J. W. Moskowitz, J. Chem. Phys., 47, 3491 (1967).

25. M. G. Griffith and L. Goodman, J. Chem. Phys., 47, 4494 (1967).

26. R. Hoffmann, J. Chem. Phys., 39, 1397 (1963).

27. F. H. M. Faisal, private communication.

TABLE 1

COMPOUNDS IRRADIATED AT 77°K GIVING THERMOLUMINESCENCE

Compound	Observed Intensity
Acridine	Strong
Adenine	Strong
Anthracene	Weak
Ascorbic acid	Weak
Benzimidazole	Strong
Benzotriazole	Weak
5-Bromoindole	Strong
5-Bromouracil	Strong
Cytosine	Strong
DNA	Weak
Eosin-Y	None
Fluorescein	None
Guanine	Weak
Hematoporhorin	Weak
L. histidine	Weak
Indole	Weak
Imidazole	Weak
Indazole	Weak
5-methylcytosine	Weak
1, 10-phenanthroline	Weak
Purine	Strong
Pyrazole	Weak
Pyronine B	None
Pyronine Y	Strong
Sodium chloride	Weak
Sucrose	Weak
Tetraphenyl pyrrole	Weak
Thionine	Weak
Triphenyl amine	Strong
2, 4, 5-triphenyl imidazole (T Pl)	Weak
Thymine	Weak
Uracil	Weak
Xanthine	Weak

(All compounds had blue emission, except TPl which appeared yellow dose approx. 3 x 10^5 rads).

ESR OF GAMMA - IRRADIATED CYTOSINE

$g = 2.02$

16 g

20 gauss
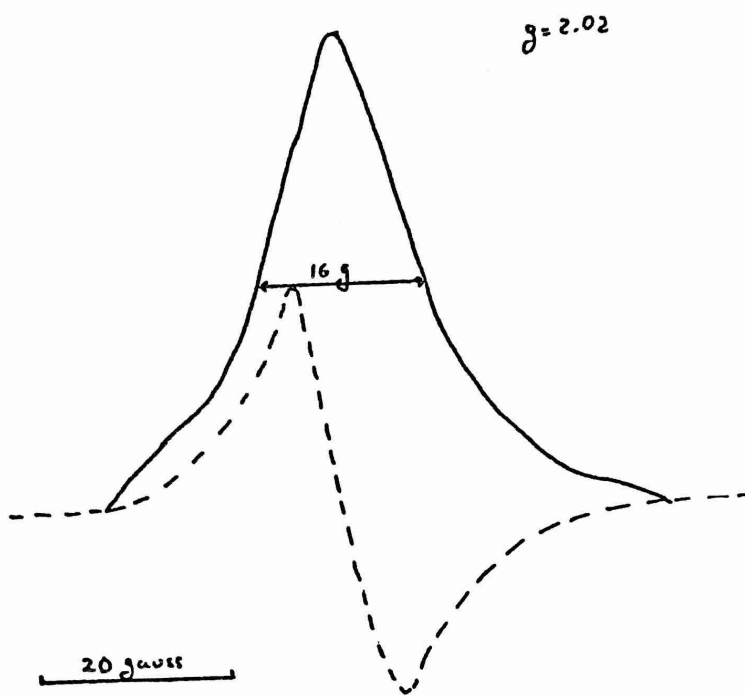
Figure 1   ---Derivative Spectrum

ESR OF GAMMA IRRADIATED URACIL

$g = 2.02$

19 g

20 gauss
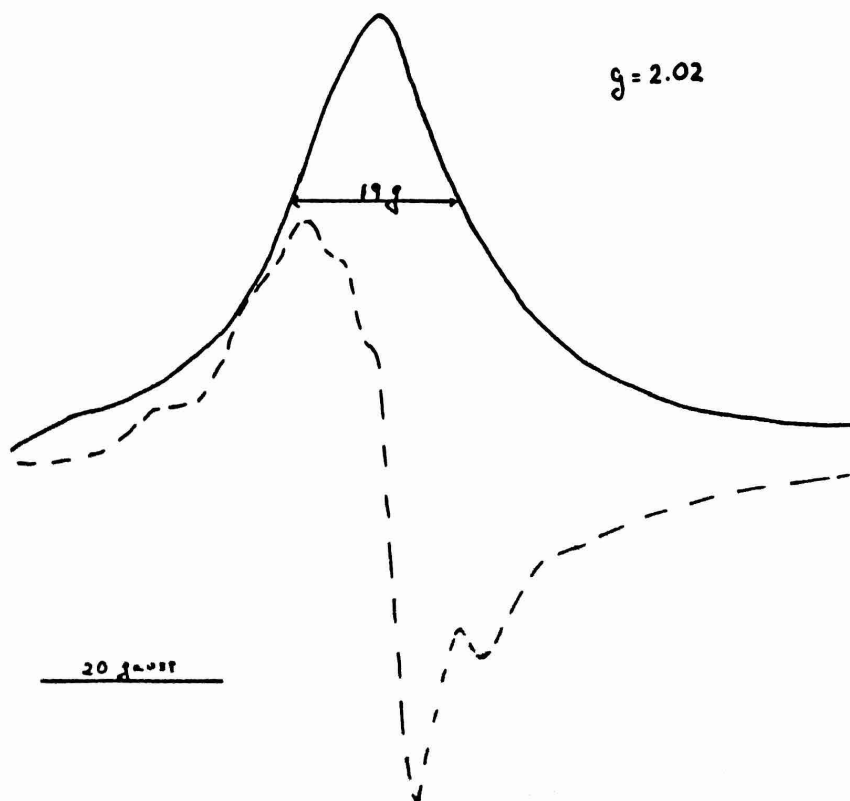
Figure 2

TABLE 2

INSTRUMENT DESCRIPTION FOR FIGURES 3, 4 AND 5

A. General Electric AH6 high pressure mercury arc
B. Arc power supply
C. Ni-Co solution filter
D. Baird Atomic interference filter 254 nm
E. Slit
F. Photographic shutter
G. Dewar box
H. Quartz dewar
I. 1 cm quart solution cell
J. Stroboslave 1539A flash lamp
K. Flash power supply and trigger unit
L. Bausch & Lomb 603AB high intensity grating monochromator
M. Wavelength drive unit
N. Emi 9526B photomultiplier
O. Fluke 412B high voltage power supply
P. Keithley 610B electrometer
Q. Leeds & Northrup 10 mV recorder
R. Tektronix 561A oscilloscope
S. RG-1000 Jena filter
T. Boxter Corp. 5900 variable intensity tungsten lamp
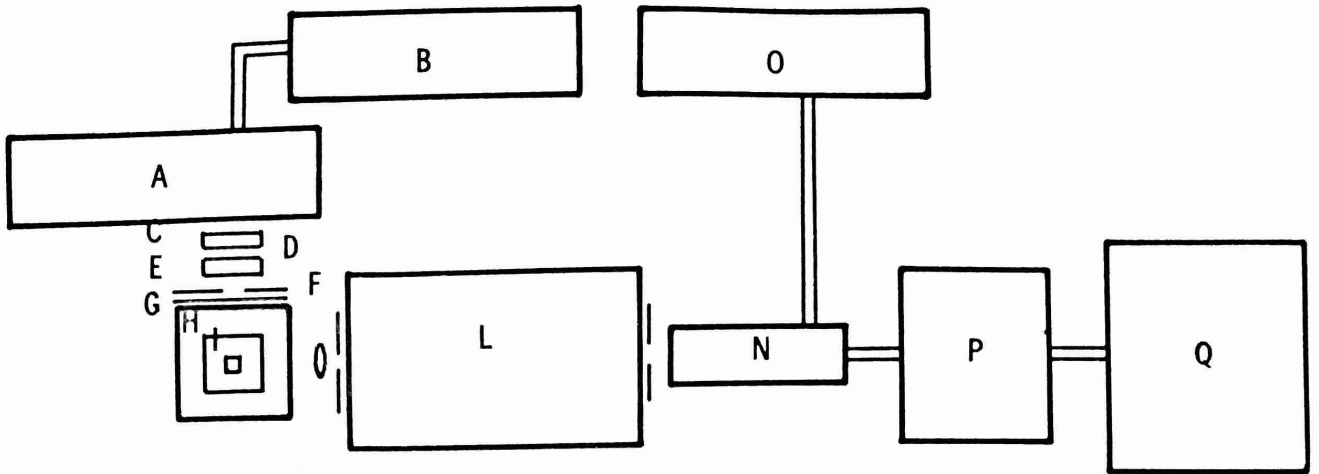
Figure 3
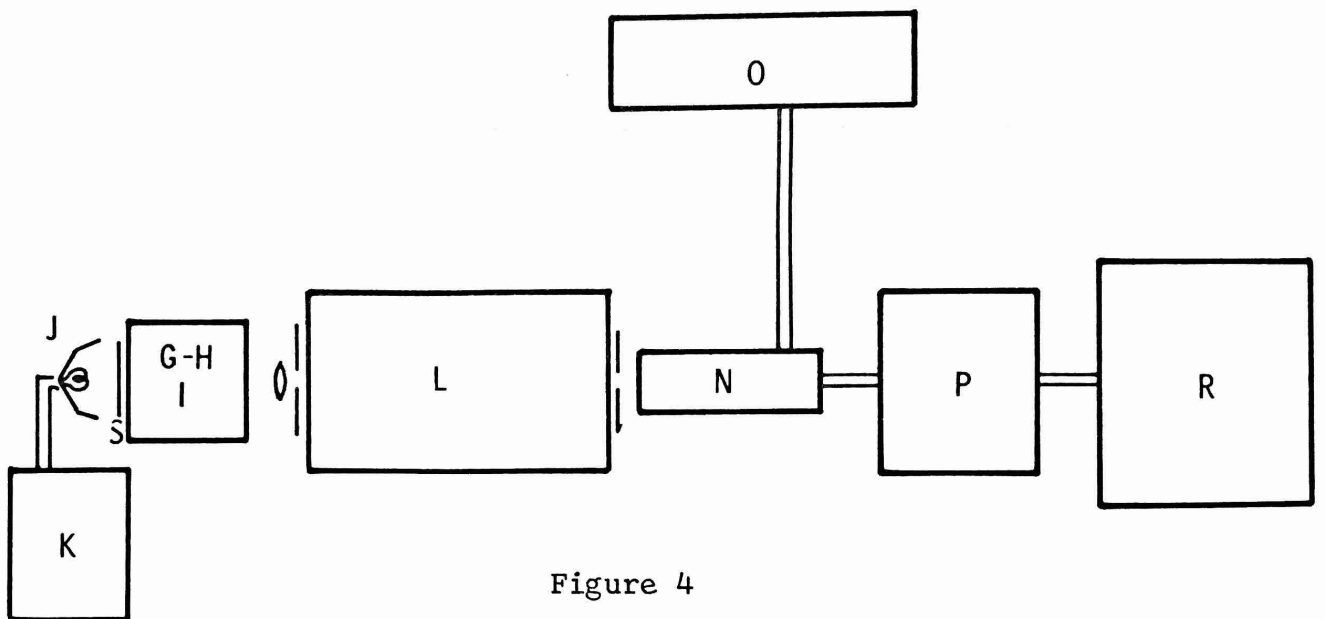
Figure 4
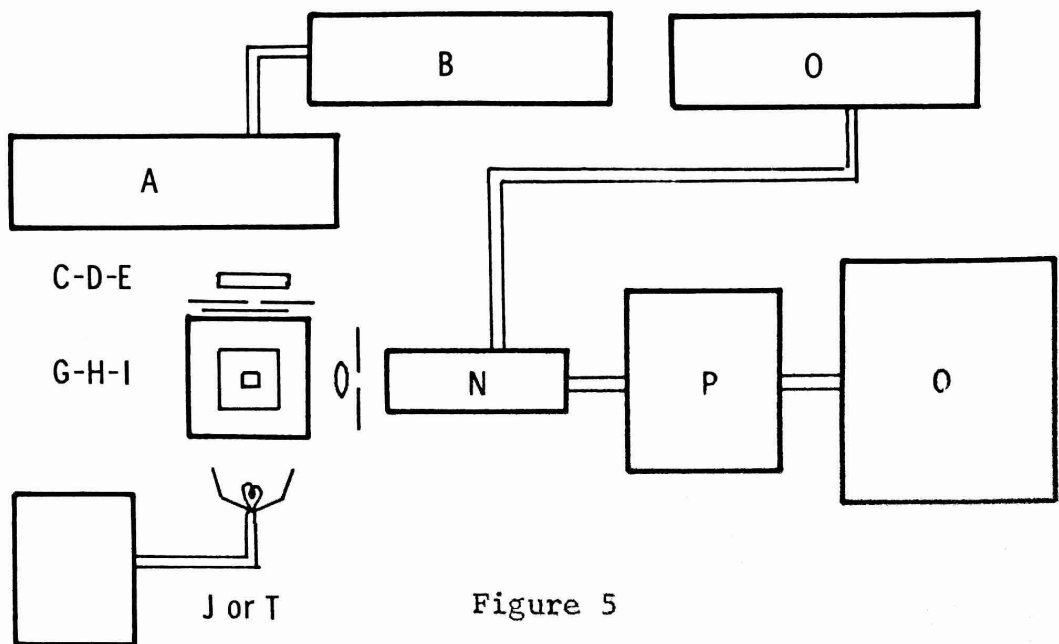
Figure 5
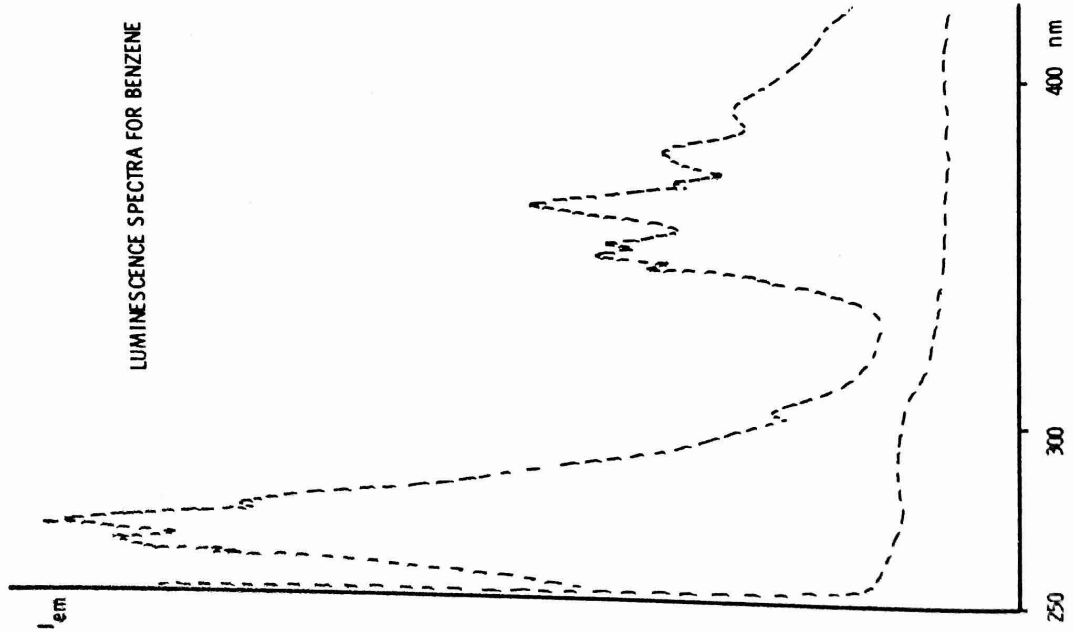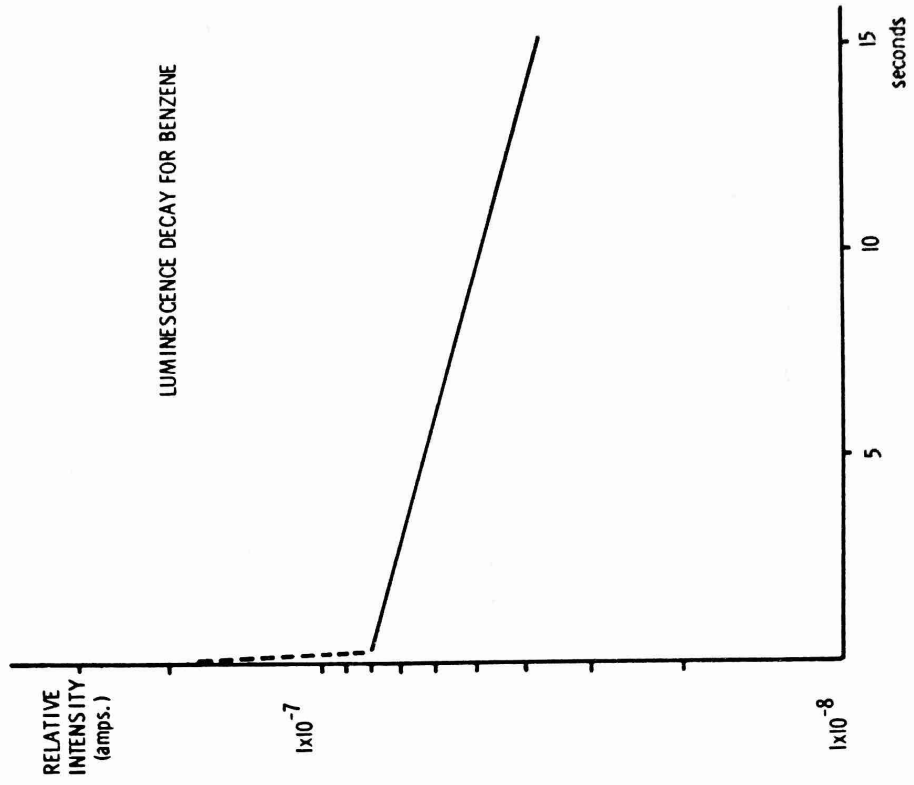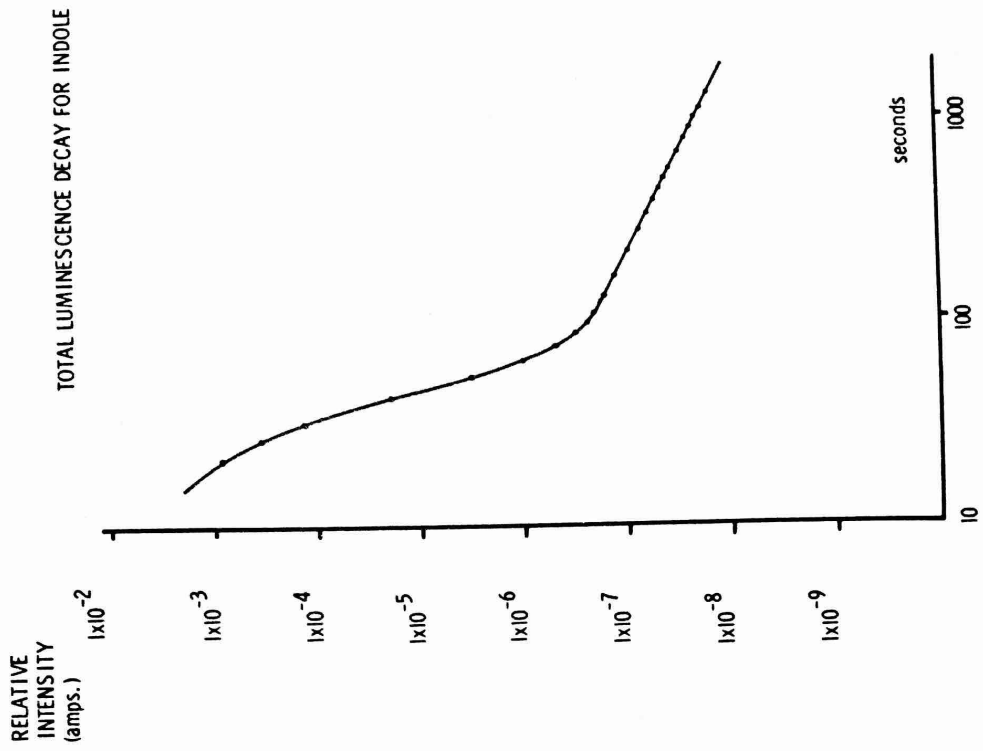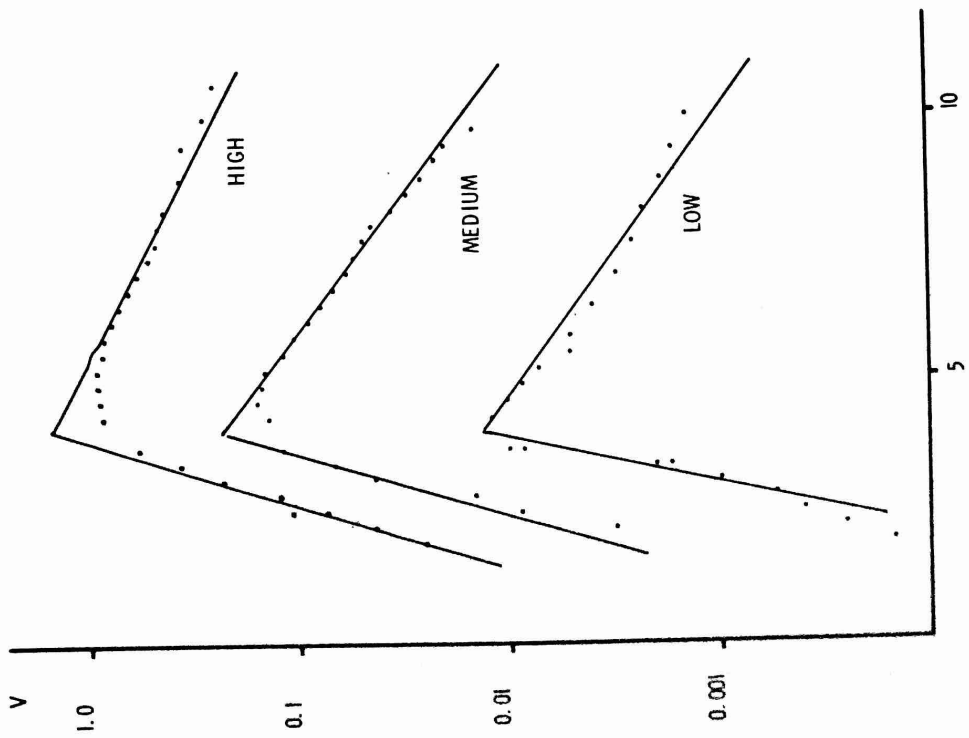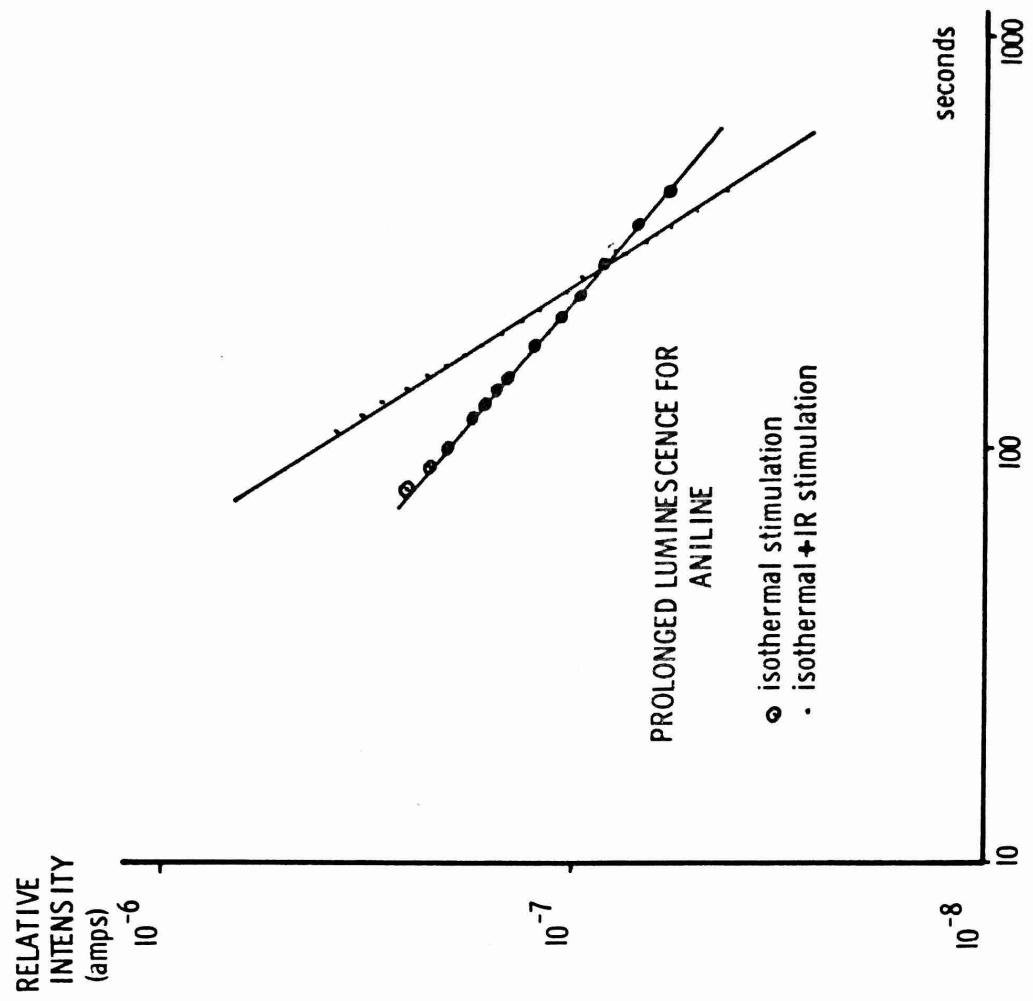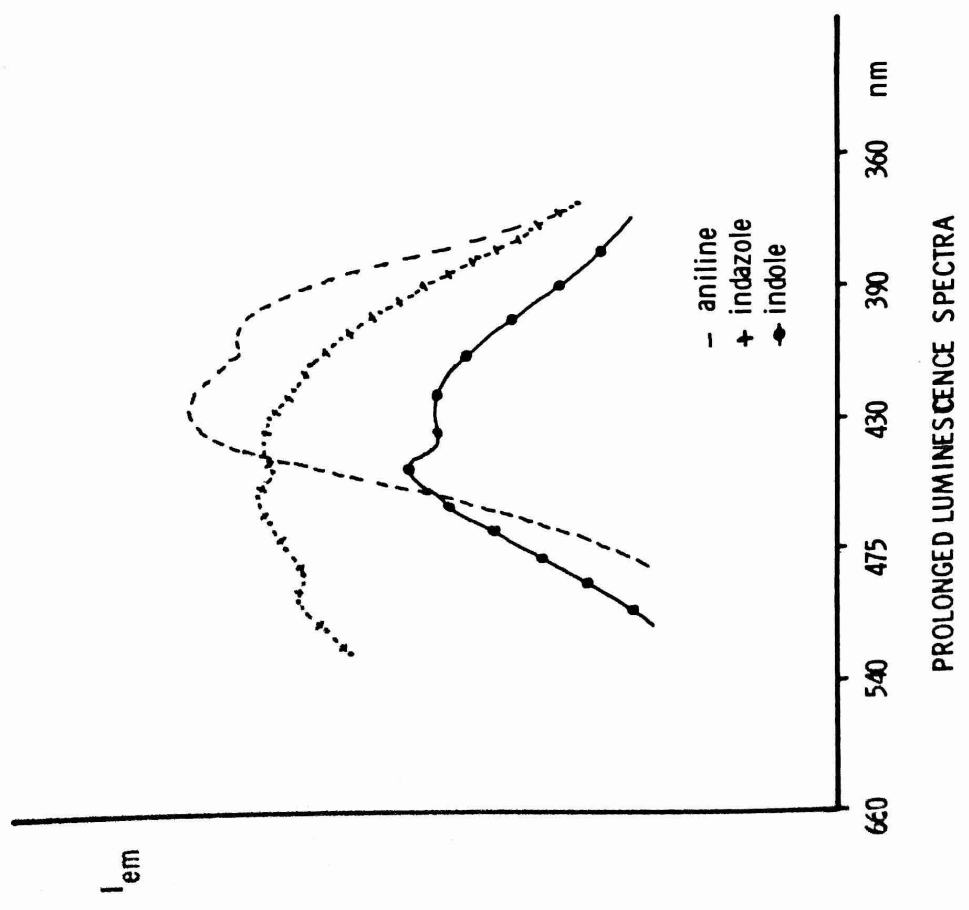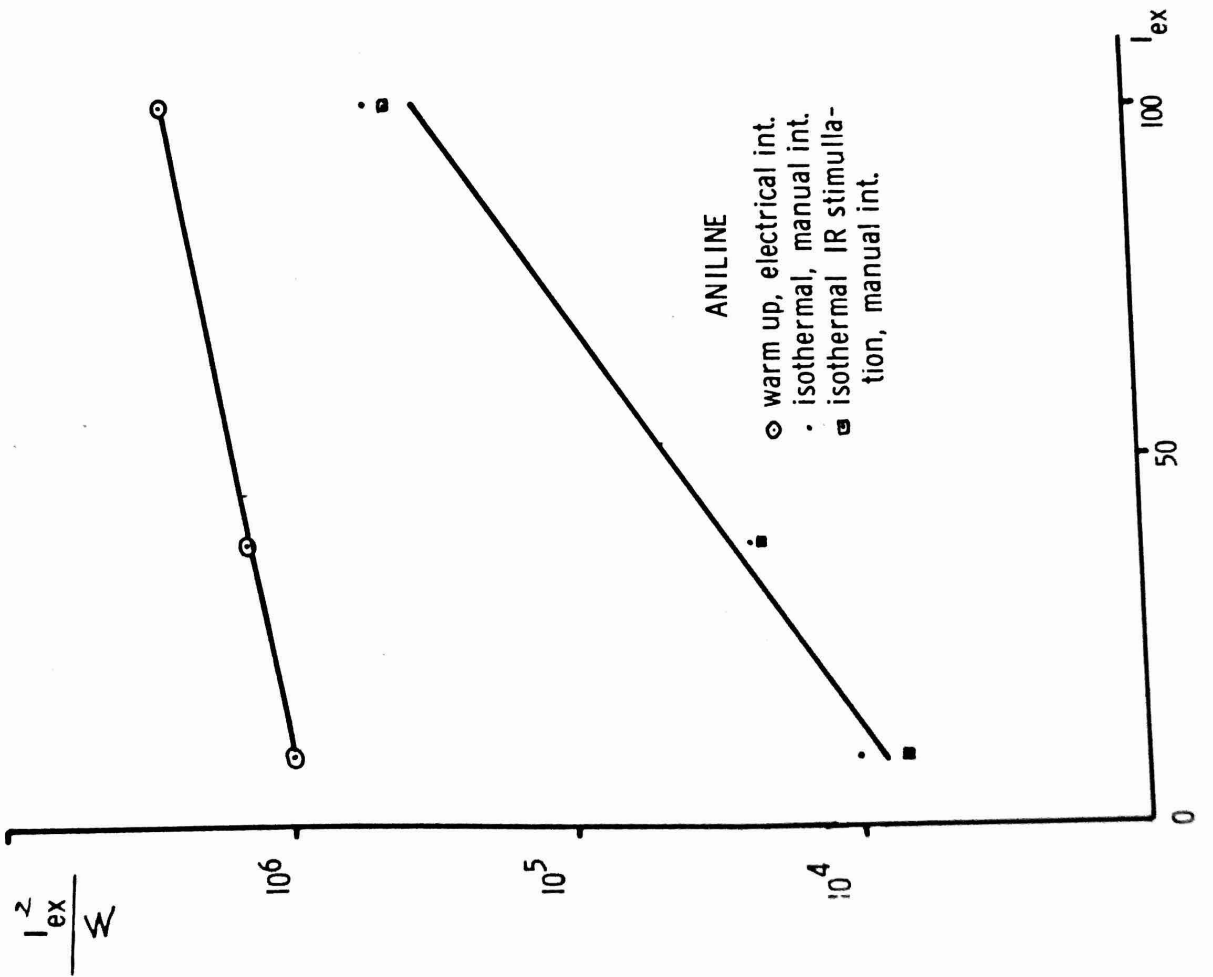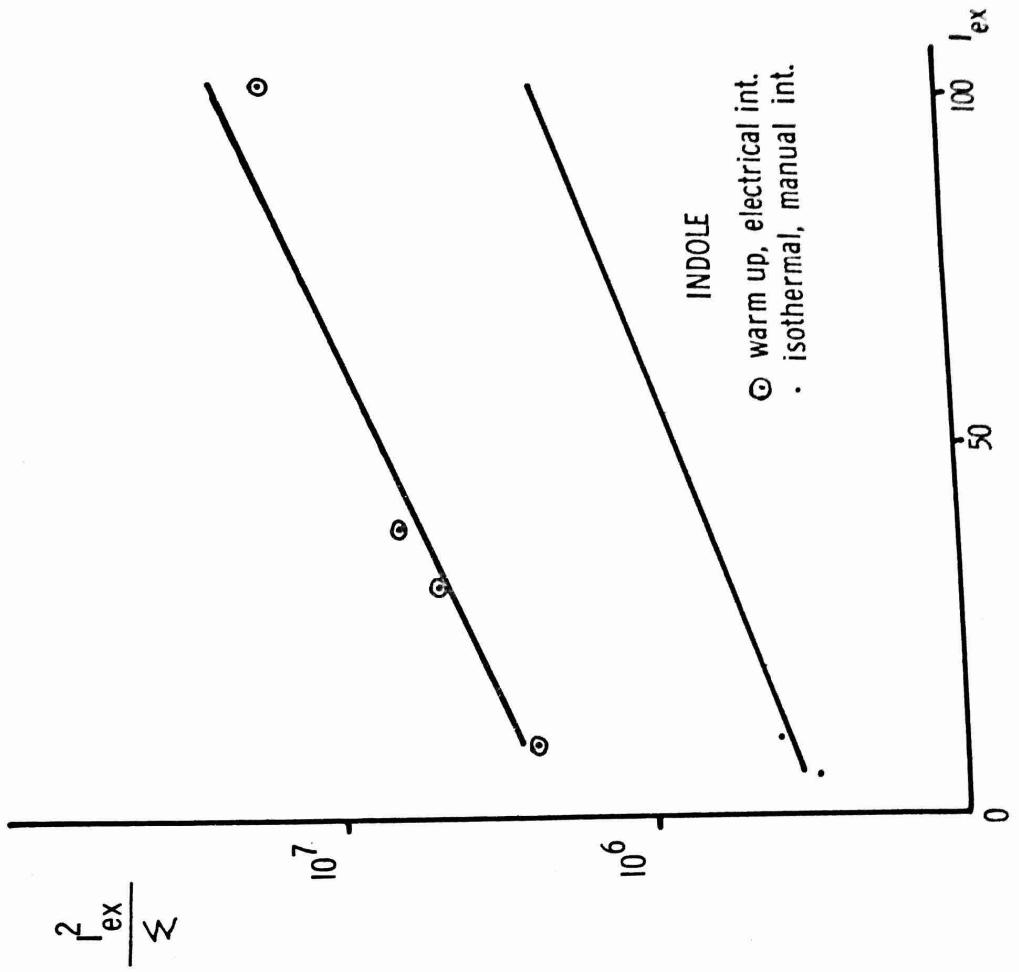
LUMINESCENCE DECAY FOR BENZENE

Figure 7

LUMINESCENCE SPECTRA FOR BENZENE

Figure 6

TOTAL LUMINESCENCE DECAY FOR INDOLE

Figure 9

Figure 8

RELATIVE
INTENSITY
(amps)

PROLONGED LUMINESCENCE FOR
ANILINE

⊙ isothermal stimulation
· isothermal + IR stimulation

Figure 11

PROLONGED LUMINESCENCE SPECTRA

− aniline
+ indazole
♦ indole

Figure 10

Figure 13

Figure 12

APPENDIX 1

ELECTRON ATTACHMENT BY PYRIDINE AND THE DIAZINES IN γ-RADIOLYSIS: EXPERIMENTAL AND THEORETICAL CONSIDERATIONS*

A. Grimison, G.A. Simpson, M. Trujillo Sánchez, and J. Jhaveri
Puerto Rico Nuclear Center,** and Departments of Chemistry and
Physics, University of Puerto Rico, San Juan, P.R., 00935

Abstract:- Absorption spectra characterizing the radical
anions of pyridine, pyrimidine, pyrazine and pyridazine have
been produced by γ-radiolysis of the parent compounds in a
2-methyl-tetrahydrofuran matrix at 77°K. These spectra are in
good agreement with those obtained by chemical reduction or
electrolysis, but some additional transitions at longer wave-
lenths have been observed. Pariser-Parr-Pople calculations of
the theoretical doublet-doublet transitions of the radical
anions yield good correlations with the experimental transitions.
The best correlation is obtained by not including configuration
interaction, at least for a very limited number of configura-
tions. Irradiation of pyridine in 3-methylpentane leads to a
thermoluminescence assigned to the phosphorescence of pyridine.

Our primary interest[15] in the production and characterization of ionic intermediates formed by the γ-radiolysis of heterocyclic molecules. This identification can provide important information on the effects of radiation on biological systems. The technique being used is that of isolation in a solid matrix at liquid nitrogen temperature.[1] From the

1) A. M. Bass and H. P. Broida, "Formation and Trapping of Free Radicals", Academic Press, New York (1960).

chemical viewpoint, perhaps the most intruiging aspect of such work is the extreme simplicity of the final processes forming these intermediates. Thus the work of Hamill and co-workers[2] has indicated how radical anions

2) M. R. Ronayne ___, J. P. Guarino and W. H. Hamill, J. Am. Chem. Soc., 84, 4230 (1962).

can be formed by attachment of low energy electrons to solute molecules. Radical cations can apparently be produced by a simple positive charge exchange between the matrix and the solute molecule.[3,4] In a previous

3) T. Shida and W. H. Hamill, J. Chem. Phys. 44, 2369 (1966).
4) A. Grimison and G. A. Simpson, J. Phys. Chem. 72, 1776 (1968).

publication,[4] we have described one radiolytic technique suitable for the production and stabilization of radical cations. By this means, absorption maxima measured at 77°K were assigned to the radical cations of pyridine, pyrrole, and thiophene.[4] In general, the production of radical anion intermediates is experimentally much less difficult. Thus

Hush and Hopton have reported the absorption spectra of the radical anions of

pyridine, pyrazine, pyrimidine, and pyridazine, produced by reduction with

sodium metal in tetrahydrofuran at room temperature.[5,6] Kimmel and Strauss[7]

---

5) J. W. Dood, F. J. Hopton, and W. S. Hush, Proc. Chem. Soc. (London)
   61 (1962).
6) F. J. Hopton, Ph.D. Thesis, University of Bristol, England (1962).
7) P. I. Kimmel and H. L. Strauss, Abstract of Papers, American Chemical
   Society Meeting, San Francisco, March 31 to April 5, 1968, S-151-,
   and private communication from H. L. Strauss.

---

reported the optical spectra of the same radical anions, produced by

electrolysis in liquid ammonia solutions. The observation of a λmax at

330 nm from alkali metal solutions in anhydrous pyridine at room temperature

is in good agreement with the earlier reports for the pyridine anion.[8]

---

8) C. D. Schmulbach, C. C. Hinckley, and D. Wasmund, J. Am. Chem. Soc.
   90, 6600 (1968).

The present paper describes our results on the effects of γ-irradiation

on the optical spectra of pyridine and the diazines in organic glasses

at 77°K. The major process observed under these conditions is shown to

be the attachment of an electron to the neutral azine molecule to form

the radical anion. The experimentally observed optical transitions from

the different experimental techniques are shown to be in excellent accord.

Finally, the semi-empirical theoretical excitation energies for the

radical anions, calculated by us, by Hush and Hopton,[6] and by Kimmel and

Strauss[7] as compared with the experimental values.

Experimental Techniques :

Pyridine, Eastman Spectrograde, was distilled from barium oxide before use in absorption spectra determination. For emission studies pyridine solutions were prepared either from the distilled pyridine or from a middle fraction of the main peak of samples injected on a 6 ft. GLC column of Carbowax 20 M at 80°C. Good separation of pyridine and its luminescent impurity, pyrazine [9], were achieved under these conditions.

---

9) C. J. Brealey, J. Chem. Phys. 24 , 571 (1956).

Pyrazine, pyridazine, and pyrimidine were best commercial grade, and were used without further purification. 2-Methyltetrahydrofuran (MTHF) was purified by passage over alumina, and stored under vacuum in a storage vessel containing Na-K alloy. 3-Methylpentane (MP) , Phillips Research Grade, was passed over a silca gel column, then stored under vacuum over Na-K alloy. Solutions of required concentrations were prepared from these purified solvents on the vacuum line by standard techniques.

γ-Irradiations were performed in the PRNC 2700 curie Co-60 source, using the Fricke technique for dosimetry.

Absorption spectra were obtained with the apparatus and techniques described previously.[4] Optical bleaching was effected with a 250 watt quartz-iodine lamp and appropriate transmission filters. Emission spectra under thermal stimulation were obtained either with an Aminco-Bowman spectrophotofluorimeter operated with a 100 nm band pass and a 1p28 photomultiplier, or a motor driven Bausch and Lomb " High Intensity " monochromator (No. 33-86-25) at 50 nm band pass and an EMI 9526B photomultiplier. The sample cell and optical dewar were permitted

to warm up in the spectrophotofluorimeter by removing the liquid nitrogen. Emission spectra were then obtained by repeated scanning of the spectra at a rate of one scan (200-700) per minute. The heating rate under these conditions is linear during the first five minutes, at approximately 20°K/minute.

THEORETICAL CALCULATIONS:

Theoretical excitation energies and oscillator strengths corresponding to doublet-doublet electronic transitions in the azine anions have been carried out using the semi-empirical Pariser-Parr-Pople (PPP) self-consistent field technique.[10] Recent non-empirical calculations

---

10) R. G. Parr, "The Quantum Theory of Molecular Electronic Structure", W. Benjamin, N.Y., 1963.

---

on the excited states of the ethylene molecule[11] including σ-π interac-

---

11) T. H. Dunning and V. McKoy, J. Chem. Phys., 47, 1733 (1967).

---

tion have given a sorely-needed justification for the reduction of the pi-electron integrals in the PPP method below the theoretical values. This can be considered as taking account of the effect of screening of the π-electron repulsions by the σ-electron distribution. In heterocyclic molecules, there is no reason to expect the similarity between radical anion and radical cation spectra suggested for the alternate hydrocarbon systems.[12] In particular, in calculating the

---

12) H. C. Longuet-Higgins and J.A. Pople, Proc. Phys. Soc. (London), A68, 591 (1955).

---

electronic properties of the azine radical cations, some thought must be given as to whether the missing electron has been removed from a lone-pair orbital, or from a pi-orbital. However, for the radical anions, the additional electron enters a pi-antibonding orbital, so that the use of a pi-electron calculation in predicting electronic excitations is justified.

Input wavefunctions for the PPP calculation were obtained from Huckel calculations on the appropriate neutral heterocyclic molecule, using conventional parameter values. As a variant on this approach in some preliminary calculations, wavefunctions from a 10-iteration ω-technique calculation[13] on the actual radical anions were used as input

---

13) A. Streitweiser, "Molecular Orbital Theory for Organic Chemists", John Wiley and Sons, Inc., N.Y., 1961, p. 115.

---

to the PPP program. However, the comparative "weakness" of the ω-technique in making electron density corrections to the coulomb integrals was shown up immediately. Thus, after one iteration of the PPP calculation, identical results obtained from Huckel and ω-input wavefunctions.

The parameter values which were used in the PPP calculations are listed in Table 1. A limited configuration interaction (CI) was also carried out among the ground state and 5 excited doublet states. The diagonal and off-diagonal CI matrix elements were obtained from formulas derived using the Longuet-Higgins and Pople approximation.[12] In view of the heavy parametrization of the Pariser-Parr-method, and

the relatively limited configuration interaction,[14] it is not surprising

---

14) N. L. Allinger and T. W. Stuart, J. Chem. Phys., 47, 4611 (1967).

---

that CI actually caused a slight deterioration of the agreement between theory and experiment. The CI values are therefore not reported in this paper.

RESULTS AND DISCUSSION

PYRIDINE

The spectrum shown in Figure 1 illustrates the absorption bands produced on radiolysis of MTHF solutions of pyridine. The 1200 nm band corresponds to the position of the trapped electron band in pure MTHF. The band at 340 nm is characteristic of pyridine in MTHF. Liberation of electrons by photolysis into the trapped electron band is expected to increase authentic radical anion absorption bands, as the liberated electrons are captured by unreacted neutral solute molecules.[2] Bleaching the trapped electron band in irradiated pyridine-MTHF solutions causes an increase in the band near 340 nm, as shown in Figure 1. Addition of 2×10^{-2} trifluoroethanol, an electron scavenger, to the pyridine-MTHF solution prior to irradiation results in the non-appearance of the 340 nm band. Figure 2 shows the dependence of the absorption at 340 nm and at 1200 nm on the initial pyridine concentration. The net absorption at 1200 nm falls off very sharply with increasing pyridine concentration, reaching a limiting (but non-zero) value at about 1×10^{-2} M pyridine. This suggests that the efficiency of pyridine for competing for electrons against solvent traps is fairly high. Simultaneously the 340 nm absorption decreases, but reaches a limiting

value at a greater pyridine concentration. This is due to a decrease

in the underlying trapped electron and associated methyltetrahydrofuranyl

radical[15] absorptions in the 340 nm region, counteracted by a build-up

---

15) F.S. Dainton, and G. A. Salmon, Proc. Soc., London A. 285, 319 (1965).

---

in the pyridine 340 nm absorption. At concentrations greater than

4×10^{-2}M, a component of the absorption can also be observed with a

maximum at 500 nm. Only in the concentration region 8×10^{-3} to

4×10^{-2}M does bleaching the trapped electron band result in an increase

in the 340 nm band.

The fact that the 340 nm band can be increased on bleaching

the trapped electron band, and is decreased on addition of an electron

scavenger, demonstrates the presence of an anionic intermediate of

pyridine. This is believed to be the pyridine radical anion, formed

by the attachment of an electron to pyridine. The assignment of the

340 nm band to the pyridine radical anion is supported by a number of

independent observations, discussed below. However, the fact that an

increase in the 340 nm absorption following trapped electron bleaching

does not occur at high pyridine concentrations requires some discussion.

One explanation is to assume a weak optical transition of the pyridine

anion at wavelengths greater than 1000 nm, which can give rise to a

photo-ejection process. Thus, the bleaching process at pyridine con-

centrations greater than 4×10^{-2}M would cause two competing processes,

capture of electrons released from matrix traps, and photo-ejection from pyridine anions. Where there is a low trapped electron yield, the photo-ejection process dominates the capture of trapped electrons released by photostimulation, and a decrease in the 340 nm absorption results. Supporting evidence for the existence of a long wavelength transition of the pyridine anion may be taken from the appearance of the limiting concentration yields of the trapped electron band in Figure 2. The non-zero value of the absorption suggests that the extinction co-efficient of the pyridine anion at 1200 nm may be as high as 20% of the value at 340 nm.

To confirm the assignment made in MTHF, and to investigate possible emission from irradiated samples, a series of studies were made in a 3-methylpentane (MP) matrix at 77°K. The advantages in using this matrix are that the trapped electron band occurs at a longer wavelength (1,700 nm), and that recombination luminescence has been observed.[16,17,18]

---

16) D. W. Skelly and W. H. Hamill, J. Chem. Phys., 43, 3497 (1965), and W. H. Hamill, private communication.
17) A. Déroulède and F. Kieffer, Nature 215, 1475 (1967).
18) M. J. Caperon, J. Bullot, A. Déroulède, and F. Kieffer, Compt. Rend. Acad. Sci. Paris, 264, 1013 (1967).

Figure 3 shows the absorption spectrum at 77°K following radiolysis of pyridine in MP glass. In addition to the trapped electron band, absorption maxima are observed near 1200 nm and at 360 nm, with an inflection near 500 nm. All of these bands disappear on warming the sample. If the sample is allowed to decay isothermally in the dark for 8 hours, the trapped electron band is reduced to less than 10% of the original value.[19]

19) J. B. Gallivan and W. H. Hamill, J. Chem. Phys. 44, 1279 (1966).

Simultaneously the bands at 1200 and 360 nm become more pronounced, as shown in Figure 3. The absorption at 1200 nm after decay, which are clearly in excess of 10% of the original absorptions, confirm the existence of a long wavelength transition of a pyridine intermediate, suggested earlier. The failure of the 360 nm band to increase after escape of trapped electrons suggests the presence of an additional intermediate which acts as an electron scavenger in the MP matrix.

Some preliminary luminescence observations of the pyridine MP system may be reported here since they are pertinent to the discussion of pyridine intermediates and are novel in their significance. On warming solutions of irradiated pyridine-MP glasses luminescences were observed. In addition to the solvent emission band at 425 nm,[20] a

20) M. Burton, M. Dillon, and R. Rein, J. Chem. Phys. 41, 2228 (1964).

structureless emission band at 365 ± 10 nm was observed, lasting up to 10 minutes after removal of the liquid nitrogen. This emission band was absent in pure MP glasses. Use of GLC purified pyridine gave the same result. The warm up luminescence obtained from an irradiated MP glass containing pyrazine, the luminescent impurity in pyridine,[9] had a maximum at 380 ± 5 nm. Phosphoresce of pyrazine occurs near 380 nm.[21] Therefore, the emission observed with pyridine-MP glasses

21) L. M. Logan and I. G. Ross, J. Chem. Phys. 43, 2903 (1965).

is associated only with pyridine and not a contamination. The wavelength corresponding to the maximum of pyridine phosphorescence can be estimated from the oxygen perturbed singlet-triplet absorption spectra to be greater than or equal to 337 nm.[22] Thus, the emission may be due

---

22) D. F. Evans, J. Chem. Soc., 3385 (1957).

---

to pyridine phosphorescence following recombination reactions. The direct phosphorescence of pyridine via intersystem crossing from an excited singlet state has apparently not been reported yet. The above interpretation requires the presence of the pyridine cation radical, which we have reported previously[4] to have a λmax at solely 380 nm. The observed band at 360 nm may thus contain unresolved components of both the anion radical (340 nm) and cation radical (380 nm) absorptions. The formation of both anionic and cationic intermediates in MP has been suggested by other workers.[16] The decrease in the 360 band on decay of the trapped electron band would then be attributable to the disappearance of the cation component. The long lifetime of the observed emission band suggests that, in addition to electron-cation recombination, phosphorescence can be produced by anion-cation recombination processes at higher temperatures.

Table 2 gives a summary of the transitions attributed to the pyridine radical anion in this work, and the experimental assignments of Hush and Hopton,[5,6] and Kimmel and Strauss.[7] The agreement on the position of the near uv band is excellent, considering the very different

experimental techniques. Thus Hush and Hopton's (HH) results refer to solution in tetrahydrofuran at room temperature, and Kimmel and Strauss (KS) results refer to liquid ammonia solutions. These other workers observe additional shorter wavelength transitions which cannot be verified under our experimental procedure. The theoretically predicted doublet-doublet transitions of the pyridine radical anion are collected on the right of Table 2. Our results, which do not include CI, give high oscillator strengths as expected, but are otherwise in better accord with the experimental results. The band at 3.7 ev is calculated at 4.29 ev, whereas KS results give 3.07 ev, and HH have no corresponding band. The band observed by HH at 5.08 ev and by KS at 4.75 ev is calculated by HH at 5.23 (allowed band) ev, by KS at 5.26 ev, and by us at 5.40 ev The suspected band at 2.5 ev (500 nm) corresponds to a predicted pyridine anion absorption at 2.66 ev (HH) or at 2.25 ev (this work). Finally, our calculations alone suggest a forbidden long wavelength transition. By using the extinction coefficient of HH for the 3.37 ev band, we estimate a G value of 2.7 for the production of the pyridine anion at high pyridine concentrations.

PYRAZINE

Figure 4 shows the absorption spectrum at 77°K after γ-radiolysis of pyrazine in a MTHF glass, and the result of bleaching the trapped electron band. An absorption maximum is produced near 345 nm, and in a suitable concentration region, an increase in this absorption is produced by bleaching the trapped electron band. The concentration dependence of these bands have not seen studied extensively, but it has been observed

that the position of the λmax increases with increasing initial

concentration of pyrazine at constant dose. Specifically, a λmax

of 320 nm is found at a concentration of 1 x 10^{-4}M, which increases

monotonically with concentration to a λmax of 345 nm at a concentra-

tion of 4 x 10^{-2}M. We attribute this effect to an artifact of the

technique of determining spectra. Difference spectra are obtained

by substracting the initial glass spectrum from that after irra-

diation. This assumes no decrease in the near uv bands of the

parent heterocyclic during radiolysis. Pyrazine has been found to

have a λmax of 315 nm in MTHF, in comparison with the value of

328 nm in cyclohexane.[6,23] This marked blue shift characterizes

the n-π * nature of the transition.[23]

---

23) M. Kasha, "A Symposium on Light and Life", Johns Hopkins Univ.
Press, Baltimore, 1961, p. 31.

Thus, depletion of pyrazine at low initial concentrations

can cause shift in the apparent position of the nearby absorption of

the pyrazine intermediate. This was demonstrated further by repeated

irradiation of the same solution to successively higher doses. On

obtaining difference spectra in the usual manner, a shift in the

λmax to shorter wavelengths with increasing dose was observed. The

position of the near uv band of the radiation induced intermediate

of pyrazine is thus assigned to be equal to or greater than that

observed at the highest concentration studied. As a result of the

above observations, an absorption maximum at 345 nm is assigned to

an anionic intermediate of pyrazine. This is believed to be the pyrazine radical anion, formed by electron attachment to pyrazine. The general features of the concentration dependence of the spectra show qualitative similarities to that observed for pyridine. At high concentration ($> 10^{-2}$ M) a maximum is resolved at 500 nm. Also at these concentrations the 340 band decreases on bleaching the trapped electron band. This suggests the existence of an unobserved long wavelength transition of the pyrazine anion.

Table 3 compares the above assignment for the pyrazine radical anion with the results of HH[5,6] and KS.[7] Again there is substantial accord among the three groups of investigators for the near uv band, remembering that our experimental value represents an upper limit to the transition energy. Again the theoretical excitation energies provide a reasonable account of the observed transitions. All three calculations give excellent accord with the high energy transition near 5 eV. For the band near 3.5 eV, KS (3.15) are in good agreement, whereas our value of 4.70 eV is very high, and that of HH is very low (2.90 eV). This latter value may be related to the suggested 2.45 eV (500 nm) band, for which we calculate 2.28 eV. A forbidden long wavelength transition is predicted near 0.5 eV. By using the extinction coefficient of HH for the near uv band, we estimate a G value of 1.7 for the production of the pyrazine anion at high pyrazine concentrations.

PYRIMIDINE

Figure 5 illustrates the absorption bands produced by radiolysis of pyrimidine in MTHF at 77°K, and the result of bleaching the trapped

electron band. An absorption maximum is produced near 320 nm, which is increased by bleaching the trapped electron band for a suitable initial pyrimidine concentration. As for pyrazine, a shift was observed in the position of the λmax with increasing initial pyrimidine concentration at constant dose. This effect is again attributed to depletion of the underlying neutral pyrimidine absorption. The band is assigned a λmax of 320 nm. in MTHF at 77°K. For concentrations above 2×10^{-2} M, a further absorption band can be resolved near 400 nm.

Table 4 compares our results for the pyrimidine radical anion with those of HH[5,6] and KS[7]. Again our experimental transition energy for the near uv band is very slightly higher than the values of these other workers, for the reason explained earlier. Our theoretical calculation gives a predicted band at 4.04 eV, in better accord with the experimental value of about 3.8 eV than the result of HH (2.86 eV) or of KS (3.01 eV). For the band near 5 eV, the values of HH (5.09 or 5.47 eV), those of KS (5.36) and our value of 4.73 or 4.94 eV are all in reasonable accord with experiment. In addition, the exist.ence of a transition near 3 eV (400 nm) reported by us is supported by calculated transitions at 2.86 eV (HH),3.01 ev (KS , but may refer to the 3.8 eV band), and at 2.53 eV (this work). A virtually forbidden long wavelength transition is again predicted. Using the extinction coefficient of HH for the near uv band, we estimate a G value for the production of the pyrimidine anion of 2.1 at high pyrimidine concentrations.

PYRIDAZINE

Figure 6 shows the absorption bands produced by radiolysis of Pyridazine in MTHF at 77°K and the result of bleaching the trapped electron band. An absorption band is produced with λmax at 354 nm, whose intensity is increased on bleaching the trapped electron band. The absorption maximum at 354 nm is therefore assigned to the pyridazine radical anion. Figure 6 also shows other overlapping absorption bands at 900 nm, and between 400 and 700 nm.

The data in Table 5 indicate the excellent agreement for the near uv band of the pyridazine radical anion among the different groups. Our theoretical excitation energy of 4.54 eV does not correspond very well with the experimental value of 3.5 - 3.6 eV. The value of KS (3.20 eV) is satisfactory, but HH have no closely corresponding band. The band found by HH at 5.13 eV is satisfactorily accounted for in all three calculations. In addition, the possible existence of bands at 2-3 eV (400-700 nm) and at 1.75 eV is partly supported by a calculated band at 2.73 eV (HH) and at 2.13 eV (this work). Using the extinction coefficient of HH for the near uv band, we estimate a G value of 0.8 for the production of the pyridazine radical anion.

CONCLUSION

The results of these investigations, taken jointly with the measurement of 'authentic' radical anion spectra by two other groups of workers, demonstrate the formation of the azine radical anions in γ-radiolysis at 77°K by the electron attachment process

$$\text{Azine} + e^- \longrightarrow (\text{Azine})^-.$$
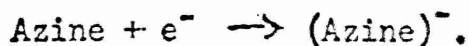
The experimental absorption spectra of the four azine radical anions

are therefore fairly well established. The reasonable accord between
the experimental transitions and the theoretical transitions, in the
π-electron approximation, confirms that the additional electron enters
a π * antibonding level. In the present calculations, no direct
account was taken of the σ-reorganization expected as a reuult of
this additional electron. We feel that specific inclusion of this
effect would provide a more adequate account of the electronic structure
of the radical anions, and are currently investigating this possibility.
The present thermoluminescence results suggest a pyridine phosphorescence
near 365 nm. If this assignment proves correct, then a fruitfull area
of spectroscopic investigation will become possible. Since many
compounds have little or no phosphorescence, such as pyridine due to its
negligible intersystem crossing efficiency,[24] production of triplets

---

24) J. Lemaire, J. Phys. Chem. 71, 612 (1967).

---

via ion recombination may well provide the only method of characterizing
the phosphorescence. Extensive work is in progress not only to substan-
tiate the pyridine emission, but also the thermoluminescence from other
non-phosphorescent compounds.

ACKNOWLEDGEMENTS

TABLE 1

PARAMETER VALUES IN PARISER-PARR-POPLE CALCULATIONS

Molecule	Coulomb and Resonance Integrals (eV)	Repulsion Integrals (eV)
Pyridine, Pyridine Radical Anion	$H_{NN} = -45.865$ $H_{22}, H_{66} = -42.535$ $H_{33}, H_{55} = -42.374$ $H_{44} = -42.343$ $H_{CN} = -2.62$ $H_{CC} = -2.29$	$(NN/NN) = 12.340$ $(CC/CC) = 11.130$ $(11/22), (11/66) = 7.770$ $(11/33), (11/55) = 5.608$ $(11/44) = 4.989$ $(22/33), (33/44), (44/55),$ $\quad (55/66) = 7.549$ $(22/44), (22/66), (33/55),$ $\quad (44/66) = 5.548$ $(22/55), (33/66) = 4.960$
Pyrazine, Pyrazine Radical Anion	$H_{NN} = -51.502$ $H_{22}, H_{33}, H_{55}, H_{66}$ $\quad = -42.706$ $H_{CN} = -2.62$ $H_{CC} = -2.29$	$(NN/NN) = 12.340$ $(CC/CC) = 11.130$ $(11/22), (11/66), (33/44),$ $\quad (44/55) = 7.776$ $(11/33), (11/55), (22/44),$ $\quad (44/66) = 5.615$ $(11/44) = 10.600$ $(22/33), (55/66) = 7.565$ $(22/55), (33/66) = 5.030$ $(22/66), (33/55) = 5.56$
Pyrimidine, Pyrimidine Radical Anion	$H_{NN} = -50.736$ $H_{22} = -42.862$ $H_{44}, H_{66} = -42.610$ $H_{55} = -42.550$ $H_{CN} = -2.62$ $H_{CC} = -2.29$	$(NN/NN) = 12.340$ $(CC/CC) = 11.130$ $(11/22), (11/66), (22/33),$ $\quad (33/44), = 7.776$ $(11/33) = 10.460$ $(11/44), (33/66) = 4.989$ $(11/55), (33/55) = 5.615$ $(22/44), (22/66), (44/66) = 5.560$ $(22/55) = 5.030$ $(44/55), (55/66) = 7.565$
Pyridazine, Pyridazine Radical Anion	$H_{NN} = -48.755$ $H_{33}, H_{66} = -42.595$ $H_{44}, H_{55} = -42.403$ $H_{NN} = -2.25$ $H_{CN} = -2.62$ $H_{CC} = -2.29$	$(NN/NN) = 12.340$ $(CC/CC) = 11.130$ $(11/22) = 10.660$ $(11/33), (11/55), (22/44),$ $\quad (22/66) = 5.608$ $(11/44), (22/55) = 4.989$ $(11/66), (22/33) = 7.770$ $(33/44), (44/55), (55/66) = 7.549$ $(33/55), (44/66) = 5.548$ $(33/66) = 4.960$

TABLE 2

TRANSITION ENERGIES (eV) FOR THE PYRIDINE ANION

Experimental values			Calculated values		
Ref. 6	Ref. 7	This work	Ref. 6	Ref. 7	This work
		~ 1.			0.26 (.000)
	2.5		2.66 (.067)		2.25 (.231)
3.7 (.078)	3.46 (.071)	3.65		3.07 (.07)	4.29 (.195)
	4.75 (.25)		5.05 (.007)		4.65 (.200)
					5.40 (.173)
5.08 (.120)			5.23 (.830)	5.26 (.007)	

Oscillator strength values in parenthesis.

TABLE 3

TRANSITION ENERGIES (eV) FOR THE PYRAZINE ANION

Experimental values			Calculated values		
Ref. 6	Ref. 7	This work	Ref. 6	Ref. 7	This work
		2.45			0.49 (.000)
			2.90 (.066)		2.28 (.188)
3.4 (.078)	3.58 (.091)	3.65		3.15 (.053)	
					4.70 (.253)
			5.16 (.215)		
4.98 (.215)	5.21 (.25)			5.22 (.113)	5.54 (.238)

Oscillator strength values in parenthesis.

TABLE 4

TRANSITION ENERGIES (eV) FOR THE PYRIMIDINE ANION

Experimental values			Calculated values		
Ref. 6	Ref. 7	This work	Ref. 6	Ref. 7	This work
					.29 (.003)
		3.1	2.86 (.081)		2.53 (.193)
3.75 (.077)	3.72 (.065)	3.9		3.01 (.169)	4.04 (.216)
4.97 (1.94)	5.11 (.25)		5.09 (.10)	5.36 (.15)	4.73 (.181)
			5.47 (.060)		4.94 (.169)

Oscillator strength values in parenthesis.

TABLE 5

TRANSITION ENERGIES (eV) FOR THE PYRIDAZINE ANION

Ref. 6	Experimental values Ref. 7	This work	Ref. 6	Calculated values Ref. 7	This work
		1.75			0.27 (.000)
		2-3	2.73 (.051)		2.13 (.168)
3.52 (.052)	3.64 (.065)	3.5		3.20 (132)	4.54 (.185)
			4.59 (.030)		4.93 (.235)
5.13 (.182)			5.24 (.062)	5.63 (125)	5.27 (.210)

Oscillator strength values in parenthesis.

Absorption spectrum of an irradiated solution of Pyridine, 2.4×10^{-2} M, in MTHF.

—— after dose of 1.6×10^{22} eV/L

-------- after 5 minutes bleach $\lambda \gtrsim 650$ nm

(Corning No. CS 2-64 filter)

Figure 1

Figure 2

Concentration dependence of absorption bands produced on radiolysis of Pyridine in MTHF .

dose = 1.9×10^{21} eV/L

O   optical density at 340 nm.

◑   optical density at 1200 nm.

Region where uv band increases on ir bleaching

Figure 3

Absorption spectrum of irradiated MP solution of Pyridine 4.0×10^{-2}M.

———— after dose of 1.2×10^{22} eV/L.

-------- after 8 hours isothermal decay.

Absorption spectrum of irradiated solutions
of Pyrazine, 1.0 x 10^{-2}M in MTHF.

——— after dose of 7.2 x 10^{21} eV/L

------ after 15 minute bleach, $\lambda > 1000$ nm.

(Schott RG-1000 filter)

Figure 4

Absorption spectra of an irradiated solution of
Pyrimidine, 5.2 x 10^{-3}M in MTHF.

——— after dose of 3.8 x 10^{21} eV/L

------ after 2 minute bleach, $\lambda > 1000$ nm.

(Schott RG-1000 filter)

Figure 5

Figure 6

APPENDIX 2

HETARYNE INTERMEDIATES

Waldemar Adam, Alec Grimison, and Roald Hoffmann[1] (Department of Chemistry and Puerto Rico Nuclear Center,[2] University of Puerto Rico, Rio Piedras, P.R., 00931, and Department of Chemistry, Cornell University, Ithaca, N. Y., 14850).

ABSTRACT:

The electronic structures of all of the possible 1, 2-, 1, 3-, and 1, 4-didehydroaromatic intermediates derived from pyridine and the diazines (hetaryne intermediates) have been calculated using the extended Hückel theory (EHT). For the didehydropyridines, it is found that of the six possible isomers, the 3,4-didehydropyridine is the most stable, and the 2, 6-didehydropyridine the least stable. Great relative stability is also predicted for 4, 5-didehydropyrazine and 4, 6-didehydropyrimidine. The complex computational trends in the hetaryne stabilities can be rationalized very well by simple molecular orbital considerations of the orbital interactions among non-bonding radical lobes and lone pair orbitals. A dominant effect is shown to be a nitrogen lone pair destabilization of nearby radical lobes. The calculated stability sequences and total electron distributions provide an excellent correlation of the available experimental data on relative stability and orientation effects in the hetaryne intermediates.

The chemistry of dehydroaromatic intermediates derived from heterocyclic molecules has been actively investigated during the last decade. Numerous papers have been published on this subject, together with extensive reviews by den Hertog and van der Plas[3], by Kauffmann[4], and by Hoffmann[5]. Principal attention has been focussed on the 1,2-dehydroaromatics derived from nitrogen heterocyclics such as pyridine, quinoline, isoquinoline, and the various diazines. These intermediates are usually formed by the dehydrohalogenation of the corresponding halogenated heterocycle on treatment with a strong base. The two adjacent radical - lobes in the 1,2 intermediates are thought to overlap appreciably, forming a partial triple bond in the heterocyclic ring. These species have been designated as hetarynes. The possibility exists, in principle, of forming 1,3- and 1,4- dehydroaromatics, in which the radical lobes are respectively in meta- and para- orientations. However, no such intermediates appear to have been reported to date. The only member of the 1,3-series that has received some attention is 2,6-dehydropyridine.[6] Here it has been postulated that conjugation through the nitrogen lone pair, which is flanked by the two radical lobes, should provide the necessary stabilization for the formation of such an intermediate.

In comparison to the dehydrobenzenes, the hetarynes are considerably more complex. While benzene can only form one 1,2- dehydro intermediate, pyridine can form either 2,3-dehydropyridine or 3,4-dehydropyridine. Of these two possible hetarynes, 3,4-dehydropyridine is formed preferentially in the dehydrohalogenation of 3-halopyridine.[7] It has only been possible to prepare 2,3-

dehydropyridine by blocking the 4-position by substitution.[8] While the symmetric dehydrobenzene intermediate gives a single product on reaction with a nucleophile, the unsymmetric 3,4-dehydropyridine can form two products, by substitution at either the 3-position or the 4-position. The preferential attack at the 4-position in 3,4-dehydropyridine provides some evidence for an important orientation effect.[3-5] Very little theoretical work seems to be available on these interesting hetaryne intermediates.[6] For this reason, we decided to examine a number of dehydroheteroaromatic molecules, using all-valence electron calculations of the extended Hückel type (EHT).[9]

THEORETICAL ANALYSIS

Extended Hückel calculations[9] on the six possible didehydropyridines result in the following stability order.

−500.23 eV   −499.74 eV   −499.69 eV

A   B   C
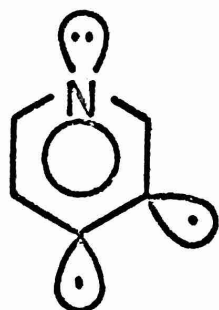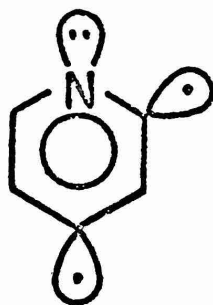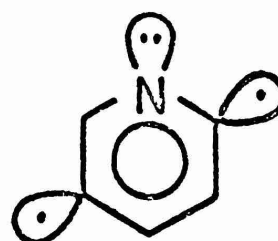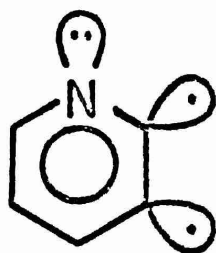
−499.41 eV   −499.31 eV   −498.53 eV
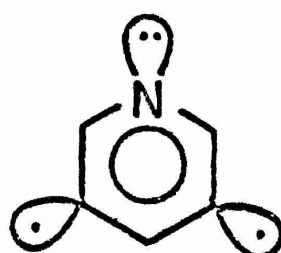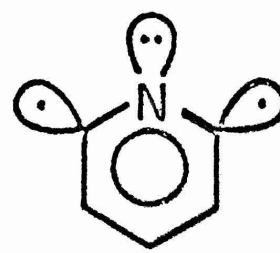
D   E   F

In contrast to a previous simple Hückel calculation, which indicated the 2,3-dehydropyridine (D) as the most stable[6], the 3,4-dehydropyridine (A) clearly emerges as the most stable isomer. The 2,3-dehydro isomer in fact is so destabilized that it appears in our calculations with a higher energy than some meta - and parahetarynes.

This agreement with one of the few experimental facts known about the hetarynes is gratifying. However, the above ordering of stabilities is initially puzzling. An explanation of this stability sequence must begin with a review of what is known of the electronic structure of the dehydrobenzenes themselves.[10] When two hydrogen atoms are removed from the aromatic ring, two orbitals may be pictured as remaining. These orbitals each formally contain one electron, and they are termed the radical lobes n_1 and n_2. The radical lobes can be combined to form wavefunctions $n_1 + n_2$ and $n_1 - n_2$, which are respectively symmetric (S) and antisymmetric (A) with respect to the two-fold rotation which interchanges n_1 and n_2. In the absence of any interaction, $n_1 + n_2$ and $n_1 - n_2$ are degenerate. Direct overlap between n_1 and n_2 (through-space) and indirect interaction with other σ and σ^* orbitals (through-bond) removes the degeneracy of the S and A molecular orbitals. The magnitude of the energy splitting between S and A is a direct measure of the quantum-mechanical interaction. It is of controlling influence as to whether the ground state of the dehydrobenzene should be a singlet or a triplet state.

The magnitude and direction of the calculated splittings were surprising.[10] Thus for ortho- and meta-benzyne we found S below A by 1.52 and 0.92 eV respectively; while for para-benzyne A was below S by 1.44 eV. These results

together with other unexpected splitting patterns led us to an interpretation of each splitting as a superposition of a direct through-space coupling and an indirect through-bond coupling. The through-space coupling always puts the positive overlap combination at a lower energy. This may be S or A depending on whether the radical lobes are in a _cis_- or a _trans_-arrangement. The through-bond coupling leads to a lower A level when the radical lobes are separated by an odd number of σ bonds, and to a lower S level when they are separated by an even number of σ bonds.[10]

We will construct two models for the analysis of the energy level patterns of the dehydroazines and dehydrodiazines. In the first model the energy levels of tridehydro- and tetradehydrobenzenes are considered initially, and the subsequent introduction of nitrogen atoms is treated as a small perturbation. The second model takes the stability ordering of the monodehydropyridine intermediates, and treats the subsequent dehydrogenation as a small perturbation.

There are three tridehydrobenzenes, each having three nearly non-bonding molecular orbitals. The tridehydrobenzenes can be labelled 123, 124, and 135 in an obvious notation, and the non-bonding orbitals designated as X_1, X_2, and X_3 in order of increasing energy, as below.
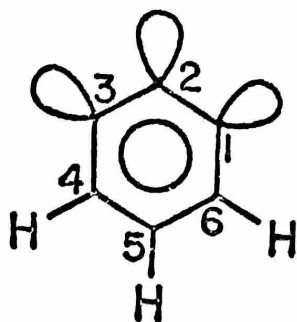
X_3 -9.99 eV   S   -9.82   eV   -10.59 eV   A

X_2 -10.59 "   A   -11.51   "   -10.59 " (e) S
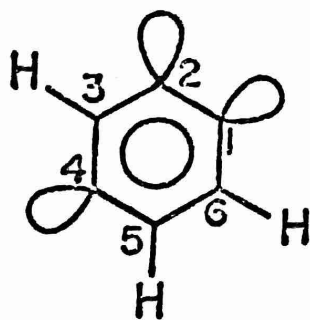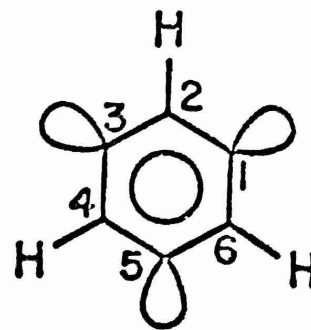
X_1 -12.56 "   S   -11.84   "   -12.53 " (a) S

The wave functions X can be classified as S or A under the two-fold rotation interchanging orbitals 1 and 3 in 123 and 135.[II] For 124 there is no two-fold axis, so that the orbitals X are simply σ-orbitals.

We would anticipate that the molecular orbitals formed from the radical lobes n_1, n_2, and n_3 in 123 should fall into a typical allylic pattern

$$X_3 \sim n_1 - c\, n_2 + n_3 \qquad S$$

$$X_2 \sim n_1 - n_2 \qquad A$$

$$X_1 \sim n_1 + c'\, n_2 + n_3 \qquad S$$

and this they do. For instance, X_1 is about 94% localized on atoms 1, 2, and 3, and has the following coefficients (z axis normal to the molecular plane and y axis along C_2 C_5)

$c_1 (2p_x)$ 0.4205 $c_2 (2p_x)$ 0.0000 $c_3 (2p_x)$ -0.4205

$c_1 (2p_y)$ 0.2000 $c_2 (2p_y)$ 0.5499 $c_3 (2p_y)$ 0.2000

$c_1 (2s)$ 0.1262 $c_2 (2s)$ 0.0474 $c_3 (2s)$ 0.1262

The molecular orbitals X_1, X_2, and X_3 of 123 can therefore be sketched as follows

$$X_1 \qquad X_2 \qquad X_3$$
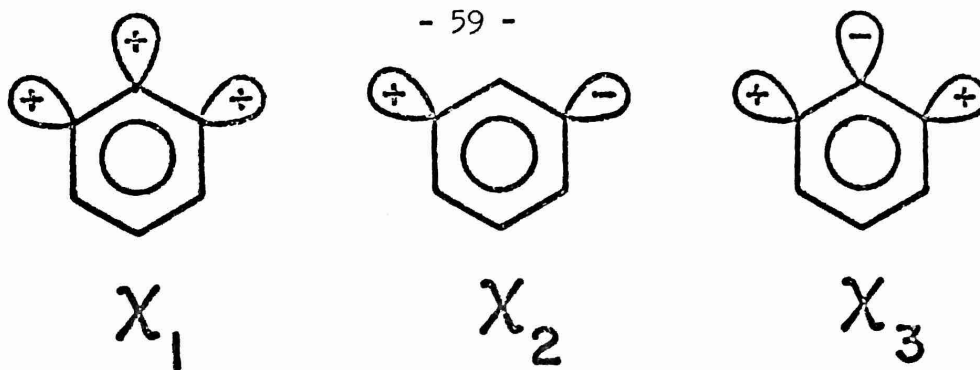
The splitting patterns found for the benzynes[10] indicated that for an _ortho_-interaction of two radical lobes the S combination was stabilized with respect to the A combination, for a _meta_-interaction the S combination was also favored, whereas for a _para_-interaction the A combination was favored. From the above diagram we see that X_1 has two favorable (S) _ortho_-interactions ($n_1 : n_2$ and $n_2 : n_3$) and one favorable (S) _meta_-interaction ($n_1 : n_3$). X_2 has one unfavorable (A) _meta_-interaction, while X_3 has two unfavorable (A) _ortho_-interactions, and one favorable (S) _meta_-interaction. By using the symbols (+·) and (−) for favorable and unfavorable interactions, we can summarize the energetics of the above interactions as

	ortho	meta	para
X_3	− −	+·	0
X_2	0	−	0
X_1	+ +	+	0

For the molecule 124 the orbitals X_1 , X_2 and X_3 are less straight-forward to construct. A logical approach is to generate the orbitals by allowing the combinations $n_1 \pm n_2$ to interact with n_4. The primary interaction is

taken as a through-bond coupling of n_1 and n_4 which places a combination $n_1 - n_4$ (A) below $n_1 + n_4$. This corresponds to the stabilization of the A combination by the <u>para</u>-interaction in the benzynes, and the fact that the <u>meta-</u>interaction between n_2 and n_4 should be much weaker. The usual interaction rule, derived from perturbation theory, is invoked - namely if two orbitals interact, the lower mixes in the upper in a bonding way,

but the upper mixes in the lower in an antibonding manner. This is shown below.
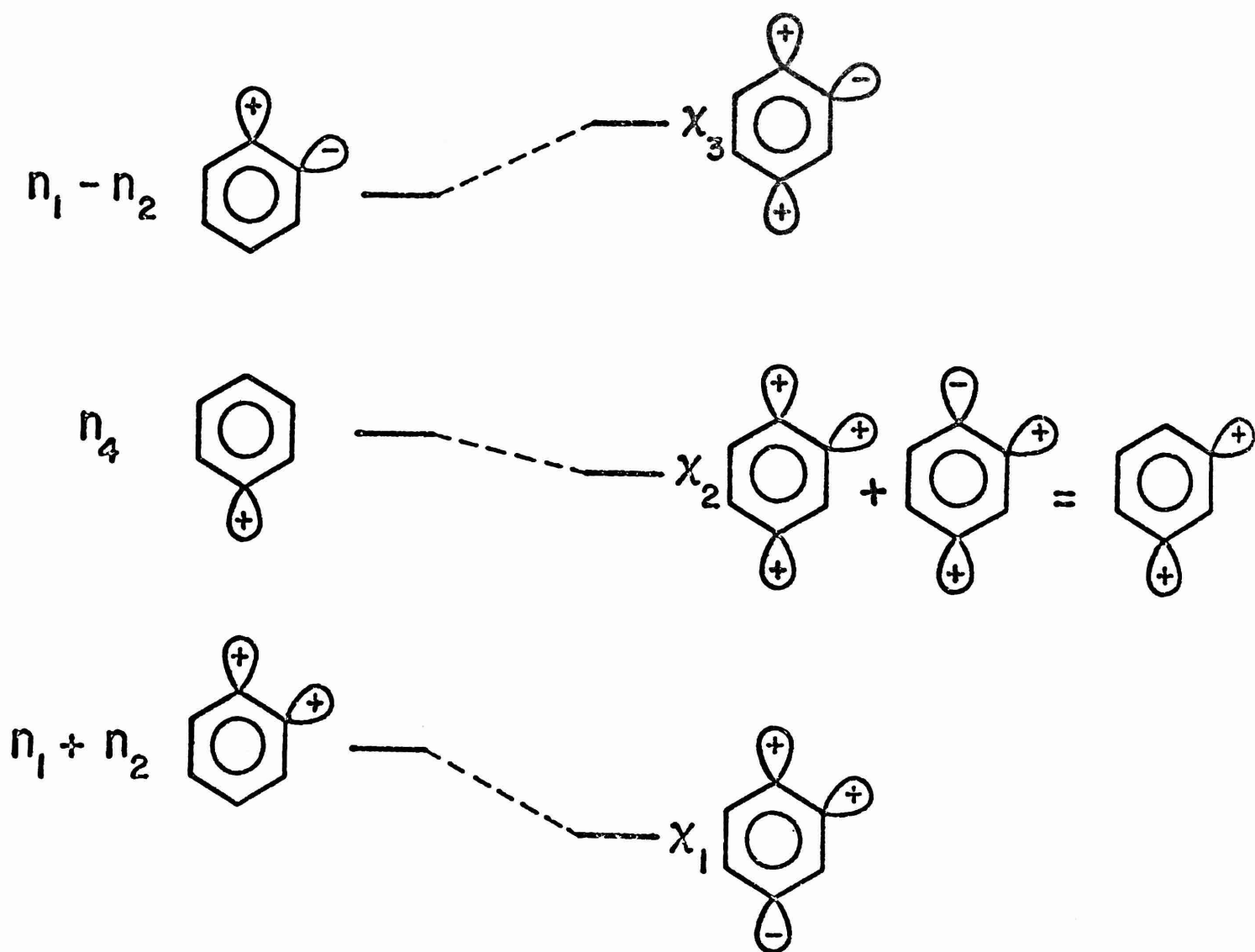
The actual molecular orbitals have the predicted composition

$$X_3 = c(n_1 - n_2) + n_4$$

$$X_2 = (c(n_1 + n_2) + n_4) + (n_4 - c(n_1 - n_2) = cn_2 + n_4$$

$$X_1 = c(n_1 + n_2) - n_4$$

The interactions may now be enumerated as was done above for the 123 system, therefore

	ortho	meta	para
X_3	−	−	−
X_2	0	+	0
X_1	+	−	+

The orbitals for 135 follow directly from symmetry. Three equivalent symmetrically disposed orbitals must interact to yield a totally symmetric combination, and a degenerate orbital pair.[12] The degenerate orbitals may be chosen arbitrarily, and the particular combination illustrated below is picked to reflect symmetry on rotation around the $C_1 - C_4$ axis.

$$X_1 \qquad\qquad X_2 \text{ degenerate } X_3$$
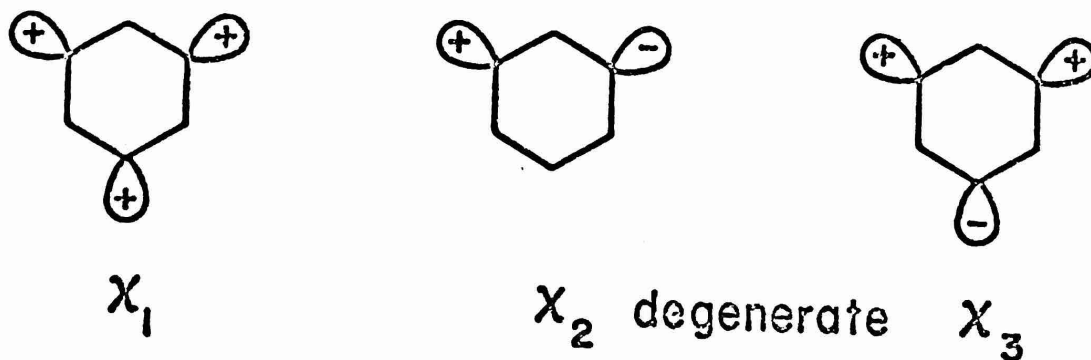
The energetics of the interactions in this case are

	ortho	meta	para
X_3	0	− (−− +)	0
X_2	0	−	0
X_1	0	+ + +	0

Referring back to the extent of the stabilization produced by the ortho-, meta-, and para-interactions in the benzynes[10] in terms of the energy splitting produced, gives E (ortho) $= 1.52$ eV, E (meta) $= 0.92$ eV, and E (para) $= 1.44$ eV. The use of these values, and the previous interaction schemes, predicts the following energy ordering for the nine orbitals of 123, 124, and 135:

$$X_1 (123) < X_1 (135) < X_1 (124) < X_2 (124) < X_2 (123) \sim X_2, X_3 (135) < X_3 (123) < X_3 (124)$$

The actual calculated energy values have been given earlier. They are in exact agreement with the above sequence, supporting the analysis of the interactions.

In the tridehydrobenzene radicals, the radical lobes are each formally occupied by one electron. Of greater significance to the present analysis are the tridehydrobenzene cations, with two electrons in the non-bonding levels, and, more importantly, the anions, with four electrons. The total computed energies for the tridehydrobenzene cations are

123	-462.81 eV
124	-461.48 eV
135	-462.06 eV

The stability ordering of these total energies is clearly in qualitative agreement with the ordering of the one-electron X_1 energies. The total energies of the tridehydrobenzene anions can be obtained from the cation energy values by adding twice the one-electron energy of the appropriate X_2 orbital. X_2 of 124 is of much lower energy than the other X_2 orbitals, so that the final anion energies

are as follows

123	-483.99 eV
124	-484.50 eV
135	-483.24 eV

The importance of the tridehydrobenzene anions is that we now suppose that the stability order is approximately preserved if the isoelectronic substitution is made of a N for a C⁻, to form the didehydropyridines.
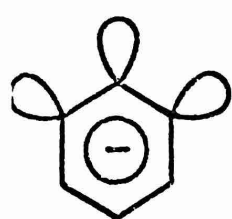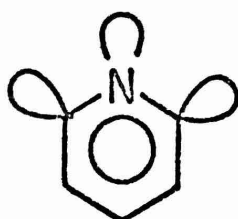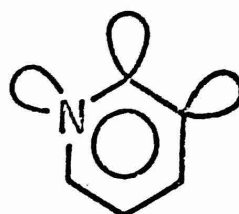
123   ⟶   F   D
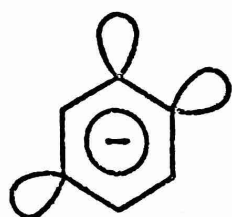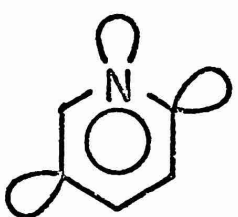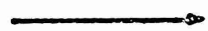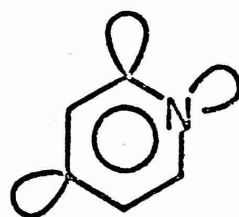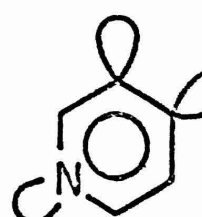
124   ⟶   C   B   A
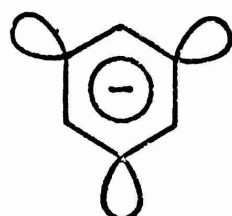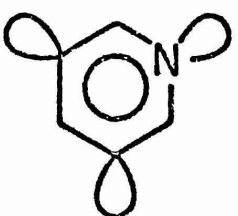
135   ⟶   E

One of the radical lobes is now formally occupied by a nitrogen lone pair. The stability ordering E (124) < E (123) < E (135) for the tridehydrobenzene anions thus implies the following grouping of the didehydropyridines, under the above assumption

$$(A, B, C) \quad < \quad (D, F) \quad < \quad E$$

A further ordering in each group can be made by simply assuming that the nitrogen preferentially enters the position of highest electron density in the tridehydrobenzene anion. For 123 and 124 these charge densities are
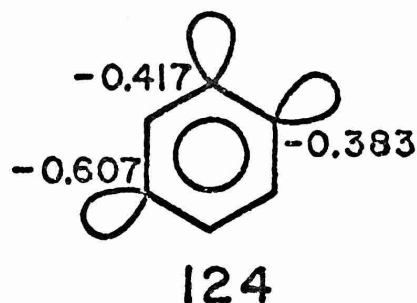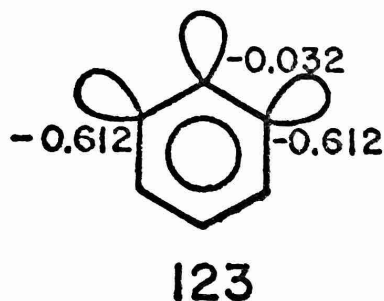
so that this would predict the ordering A < C < B < D < F < E . This is quite close to the actual alphabetical ordering obtained by the direct calculation.

We now turn to the second model for the stability sequence of the dehydropyridines. Table I below compares the energies of the $n_1 + n_2(S)$ and $n_1 - n_2$ (A) molecular orbitals calculated for the benzynes, monodehydropyridines, and diazines. In the benzynes the radical lobes are each formally occupied by one electron, in the monodehydropyridines three electrons are shared between the radical lobes, and in the diazines the 'radical lobes' are fully occupied with four electrons. For example, the ortho - series is
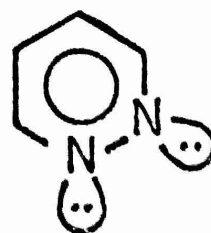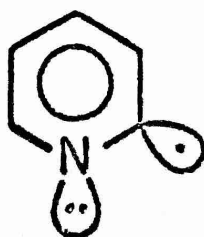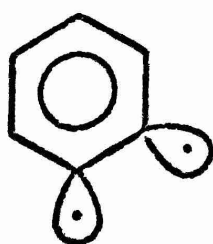
Table I: Energies (in eV) of Non-Bonding Orbitals in <u>ortho-</u>, <u>meta-</u>, and <u>para-</u>
Benzynes, Monodehydropyridines, and Diazines.

		Benzyne		Monodehydropyridine		Diazine	
ortho-		-10.19	A	-11.00	"A"	-12.40	A
		-11.71	S	-12.96	"S"	-13.39	S
	$\lvert \triangle E \rvert$	1.52		1.96		0.99	
meta-		-10.59	A	-11.16	"A"	-12.58	A
		-11.51	S	-12.78	"S"	-13.39	S
	$\lvert \triangle E \rvert$	0.92		1.62		0.81	
para-		-10.37	S	-10.83	"S"	-12.58	S
		-11.81	A	-13.24	"A"	-13.85	A
	$\lvert \triangle E \rvert$	1.44		2.41		1.67	

It should be noted that whereas symmetry requires the relation $c_1 = \pm c_2$ in the
molecular orbital $c_1 n_1 \pm c_2 n_2$ in the benzynes and diazines, there is no such
restraint for the pyridinyl radicals. If n_1 is on N and n_2 is on C, then invariably
the lower energy orbital has $\lvert c_1 \rvert > \lvert c_2 \rvert$ (considerable localization on N), and
the higher energy orbital has $\lvert c_1 \rvert < \lvert c_2 \rvert$. However, the molecular orbitals are
such that they can be identified as approximately "S" (c_1 same sign as c_2) and
"A" (c_1 opposite sign to c_2).

In all cases the ortho- and para-interactions are greater than the meta-interactions. The specific trends are not completely understood by us, though it is clear that the relative efficiency of through-space versus through-bond interaction must be involved. Particularly interesting is the greater magnitude of the splitting in the "heteronuclear" pyridinyl case over the "homonuclear" benzyne and diazine splittings. This can be attributed to the separation of the C and N orbital energies before the interaction is "turned on". In confirmation of this, we obtain large splittings in the following molecules, which are isoelectronic with the benzynes

| $|\Delta E|$ | 3.92 | 3.56 | 4.29 eV |
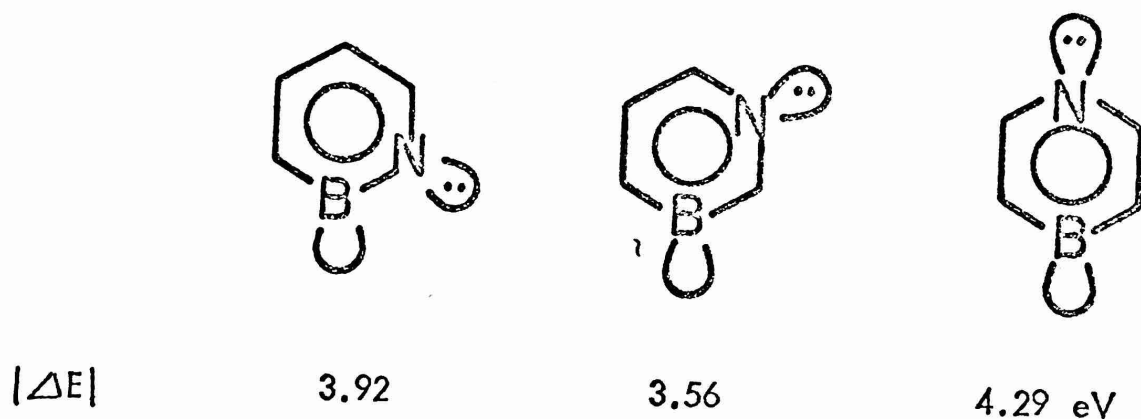
The smaller interaction of meta-oriented orbitals in the benzyne, pyridinyl, and diazine systems results in the upper molecular orbital (A in this case) being destabilized less than the upper molecular orbitals for ortho- (A) and para- (S) oriented lobes. The consequence is that when two electrons occupy the non-bonding molecular orbitals, as in benzyne, monodehydropyridinyl cation, and diazine dication the ortho-isomer (benzyne) or the para-isomer (pyridinyl, diazine) is the most stable.

However, the <u>meta</u>-isomer becomes progressively stabilized relative to the other isomers by the addition of one, and two further electrons. The actual energetics are summarized in Table 2.

<u>Table 2:</u> Total Energies (in eV) of Benzynes, Monodehydropyridines, and Diazines as a Function of the Number of Non-Bonding Electrons.

2-electron case

	benzyne	pyridinyl^{+}	diazine^{++}
o	-492.58	-507.76	-520.75
m	-491.99	-507.68	-521.45
p	-492.37	-508.17	-521.88

3-electron case

	benzyne^{-}	pyridinyl	diazine^{+}
o	-502.77	-518.75	-533.15
m	-502.58	-518.84	-534.03
p	-502.74	-519.00	-534.06

4-electron case

	benzyne^{--}	pyridinyl^{-}	diazine
o	-512.96	-529.75	-545.55
m	-513.17	-530.00	-546.61
p	-513.11	-529.83	-546.24

Our primary conclusions are based on the results for the neutral pyridinyl (3-electron) and neutral diazine (4-electron) systems. The pyridinyl results imply that a lone pair _para_ to a radical lobe is more stable than the _meta_-orientation, which is more stable than the _ortho_-orientation. The diazine results further suggest a strong destabilization of two adjacent nitrogens (lone pair repulsion?) and a stabilization of a _meta_-interaction of two lone pair orbitals.

We can now examine the didehydropyridine results in the light of the above considerations on lone pair-radical lobe interactions. The number and type of N-radical interactions in the various didehydropyridines are listed below.

N -Radical Interactions

Structure	ortho	meta	para
A	0	1	1
B	1	0	1
C	1	1	0
D	1	1	0
E	0	2	0
F	2	0	0

Taking the above stabilizing effect _para_ > _meta_ > _ortho_ , gives the energy sequence A < B < E < C,D < F . Only the order of E and C,D is inconsistent. This can be explained by the presence of a stabilizing _ortho_ radical —radical lobe interaction of the benzyne type present in C and D, but absent in E.

We now turn to the dehydrodiazines. Using idealized geometries, the eleven possible dehydrodiazines exhibit the following stability sequences:
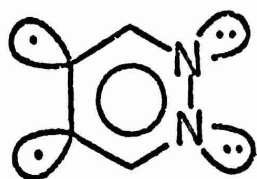
-507.55 eV

G
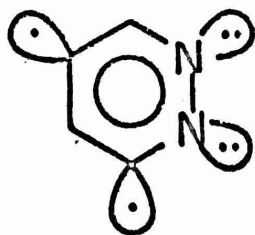
-506.83

H
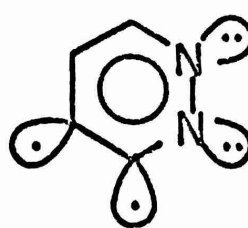
-506.74

I
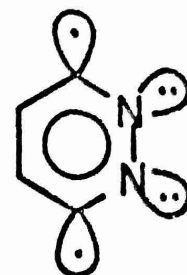
-506.63

J
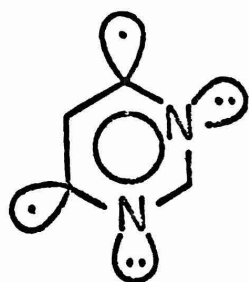
-508.10

K
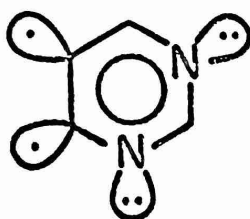
-507.87

L
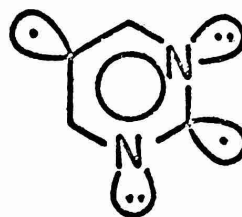
-507.39

M
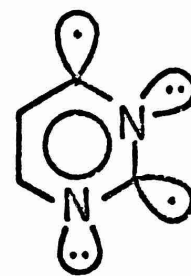
-507.05

N
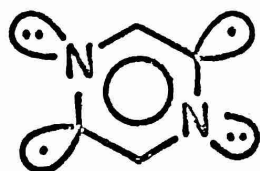
-507.57

O

-506.68

P
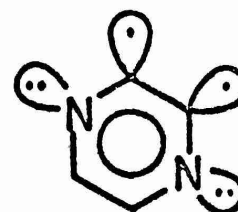
-506.43

Q

Once again the analysis is two-fold. We begin by considering the three
tetradehydrobenzenes
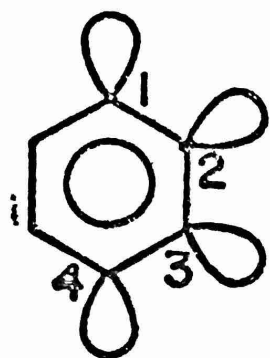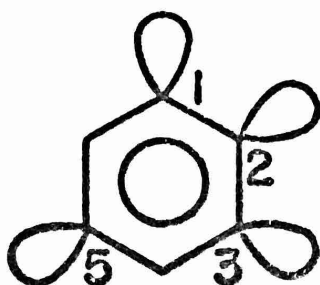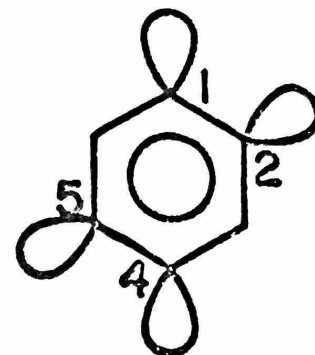
1234   **1235**   **1245**

The molecular orbitals of 1234 and 1245 are essentially determined by symmetry. We write them as ϕ_1, ϕ_2, ϕ_3 and ϕ_4 in an arbitrary order, since their final energy ordering is not obvious in every case. For 1234 the symbols S and A refer to the symmetry operation interchanging n_1 and n_4, and n_2 and n_3. For 1245 the symbols SS, AA, AS, and SA refer first to the symmetry operation interchanging n_1 and n_5, and n_2 and n_4, then to the symmetry operation interchanging n_1 and n_2, and n_4 and n_5. Note the obvious and not accidental resemblance of the orbitals of 1234 and 1245 to the π-orbitals of a butadiene.

1234
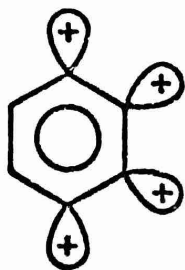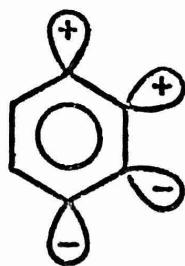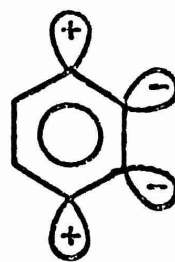
$$\phi_1 \,(S) \qquad \phi_2 \,(A) \qquad \phi_3 \,(S) \qquad \phi_4 \,(A)$$

1245
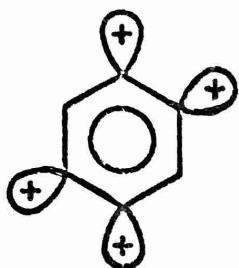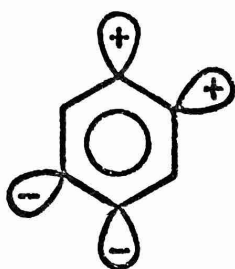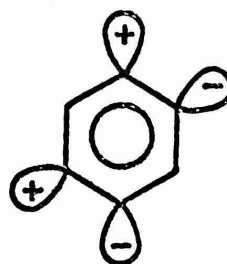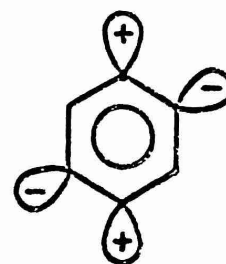
$$\phi_1 \,(SS) \qquad \phi_2 \,(AS) \qquad \phi_3 \,(SA) \qquad \phi_4 \,(AA)$$

The composition of the 1235 molecular orbitals is not easily predicted. They emerge from the calculation resembling a set of cyclobutadiene orbitals :
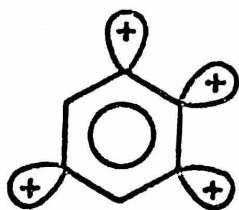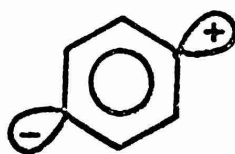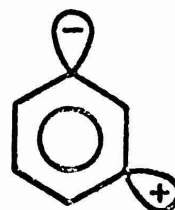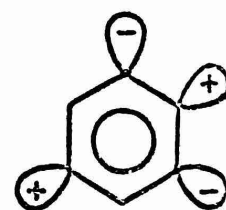
$$\phi_1 \,(S) \qquad \phi_2 \,(S) \qquad \phi_3 \,(A) \qquad \phi_4 \,(S)$$

We now estimate the favorable and unfavorable interactions for each of these molecular orbitals as was done for the tridehydrobenzenes.

			ortho	meta	para
	(A)	ϕ_4	---	++	+
	(S)	ϕ_3	-(--)	--	-
1234	(A)	ϕ_2	+(++ -)	--	+
	(S)	ϕ_1	+++	++	-
	(S)	ϕ_4	--	+	-
1235	(A)	ϕ_3	0	-	0
	(S)	ϕ_2	0	0	+
	(S)	ϕ_1	++	+++	-
	(AA)	ϕ_4	--	--	--
1245	(S A)	ϕ_3	--	++	++
	(AS)	ϕ_2	+ +	--	++
	(S S)	ϕ_1	+ +	+ +	--

Recalling that an ortho- or para-interaction is more stabilizing than a meta-interaction, we would predict for 1234 the energy ordering $\phi_1 < \phi_2 < \phi_4 < \phi_3$, for 1235 $\phi_1 < \phi_2 < \phi_3 < \phi_4$, and for 1245 $\phi_2 < \phi_1 \sim \phi_3 < \phi_4$. These conclusions are confirmed by the calculated energy level orderings (in eV),

1234		1235		1245	
-9.78	(S)	-9.58	(S)	-9.29	(AA)
-10.04	(A)	-10.59	(A)	-11.49	(SS)
-11.83	(A)	-11.78	(S)	-11.55	(SA)
-12.72	(S)	-12.76	(S)	-11.97	(AS)

The calculated total energies for the six electron systems which correspond to the tetradehydrobenzene dianions are

(1234) dianion	-475.39 eV
(1235) dianion	-476.00 eV
(1245) dianion	-476.54 eV

The stabilization of 1245 is essentially due to the relatively low energy of its highest occupied molecular orbital. In fact, the total energy order $1245 < 1235 < 1234$ is paralled by the highest occupied level energies $-11.49 < -10.59 < -10.04$, respectively.

To obtain the didehydrodiazines, we proceed to replace two carbon atoms by nitrogen atoms in the tetradehydrobenzene dianions. For each type of diazine the stability sequence presented earlier is completely predicted by the above considerations, that is

$$(1245) \quad < \quad (1235) \quad < \quad (1234)$$
$$G \quad < \quad H \quad < \quad I, J$$
$$K \quad < \quad L, M \quad < \quad N$$
$$O \quad < \quad P \quad < \quad Q$$
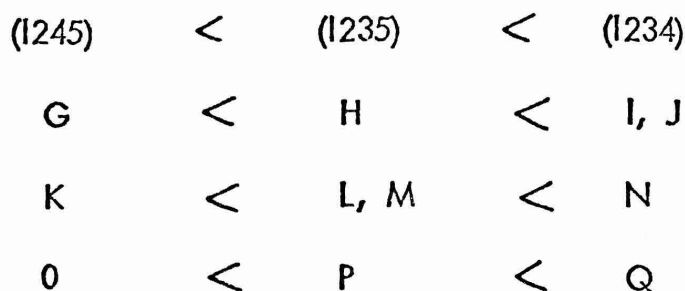
Placing all eleven isomers on a single energy scale is difficult, since relative weights would have to be assigned to the effects of radical lobe interactions and lone pair lobe interactions.

The second analysis, starting from the stabilities of the pyridinyl radicals, is quite successful in rationalizing the observed trends for the dehydropyridazines and pyrimidines (G to N), as illustrated below. However, it fails to distinguish among the dehydropyrazines where each isomer has two ortho and two meta interactions.

Structure	Nitrogen Radical Interactions		
	ortho	meta	para
G	0	2	2
H	1	2	1
I	1	2	1
J	2	2	0
K	2	0	2
L	1	2	0
M	2	2	0
N	3	0	1

We have gone into great detail in the above qualitative analysis to illus-
trate how the complex computational trends we have observed are understandable
in terms of qualitative molecular orbital arguments. In addition to the molecules
already mentioned, our actual calculations covered a number of other dehydro-
heterocyclics. The results are summarized in Tables 3-5 below, where the hetarynes
are grouped as 1-2, 1-3, or 1-4 diradicals.

Table 3: 1,2-Didehydroaromatics
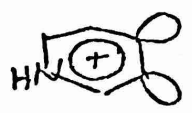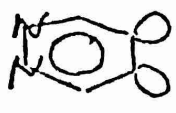
Molecule	E total (eV)	Splitting ΔE (eV)	Total Electron Densities q_α	q_β
	-492.58	1.52	4.20	4.20
	-499.77	0.86	3.77	4.25
	-500.60	1.63	4.35	3.97
	-505.95	1.11	3.94	4.10
	-506.60	1.54	4.29	3.94
	-506.74	0.89	3.98	3.91
	-507.55	1.57	4.11	4.11
	-507.87	1.04	3.55	4.44
	-505.43	0.04	3.81	3.81

Table 4: 1, 3-Dehydroaromatics
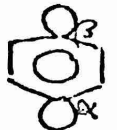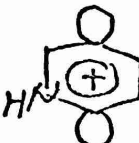
Molecule	E_{total} (eV)	Splitting ΔE (eV)	Overlap Population $P_{\alpha\beta}$	Total Electron Densities q_α	q_β
(structure)	-491.99	0.92	0.041	4.21	4.21
(structure)	-500.13	1.33	0.034	3.97	4.07
(structure)	-498.88	0.04	-0.008	3.85	3.85
(structure)	-499.72	0.69	0.047	4.18	4.18
(structure)	-505.93	1.11	0.047	4.01	3.89
(structure)	-505.29	0.59	0.001	3.87	3.87
(structure)	-505.89	0.94	0.046	4.18	4.18
(structure)	-506.83	1.15	0.039	3.90	4.02
(structure)	-507.05	0.70	-0.037	3.96	3.41
(structure)	-508.10	1.70	0.037	3.81	3.81
(structure)	-506.68	0.23	-0.173	4.06	4.06

Table 5: I, 4-Didehydroaromatics

Molecule	E_{total} (eV)	Splitting ΔE (eV)	Overlap Population $P_{\alpha\beta}$	Total Electron Densities q_α	q_β
	-492.37	1.44	-0.119	4.30	4.30
	-500.05	1.43	-0.108	3.89	4.39
	-500.99	1.28	-0.110	3.97	4.24
	-506.63	1.22	-0.098	3.87	3.87
	-507.39	1.37	-0.096	3.62	4.26
	-507.57	1.52	-0.097	3.99	3.99

Clearly the position of the nitrogen lone pairs has an effect on the energy splitting ΔE between S and A molecular orbitals. Of great interest is the fact that there is a consistent correlation between stability and the magnitude of this one-electron energy splitting. Compare, for example, the dehydropyridines in Tables 3-5. The largest splittings are associated with molecules for which we predict great relative stability. These are 3, 4-dehydropyridine, 4, 5-dehydropyrazine, and 4,6-dehydropyrimidine, which probably have singlet ground states.

## INTERPRETATION OF EXPERIMENTAL DATA

We first turn to the experimental evidence available on the stability of the 1,2 hetarynes. Treatment of a 3-halopyridine with a strong base (usually an alkylated amide ion) leads to the 3- and 4- amino-substituted pyridines, as shown in the equation below.[7]
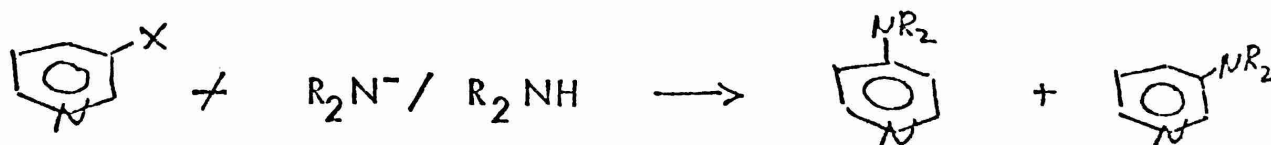
No 2-aminopyridine is observed in these reactions, unless the 4-position is blocked by an alkyl group.[8] A 3,4 -didehydropyridine must be the preferred intermediate in this reaction, rather than the 2,3-isomer. Naively, the 2,3-isomer would be expected to be more stable, since two electrons from the radical lobes, together with the nitrogen lone pair can be delocalized over three atoms. This suggestion has been forwarded, resting on the basis of a Hückel molecular orbital
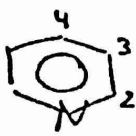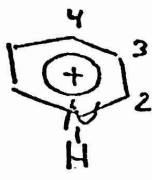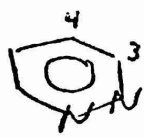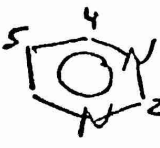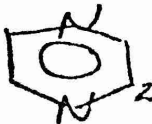
calculation.[6]   As pointed out in the theoretical analysis, our extended Hückel

calculations, which are in agreement with the experimental data, argue against

the utility of simple delocalization over the three adjacent atoms. On the con-

trary, whenever the nitrogen lone pair is adjacent to the radical lobes, we have

seen that the intermediate experiences a pronounced destabilization.

If the accepted mechanism of dehydrohalogenation of 3-halopyridines is

considered[3-5], two reasons emerge for the formation of 3-and 4-aminopyridines,

rather than 2-aminopyridine. The mechanism is
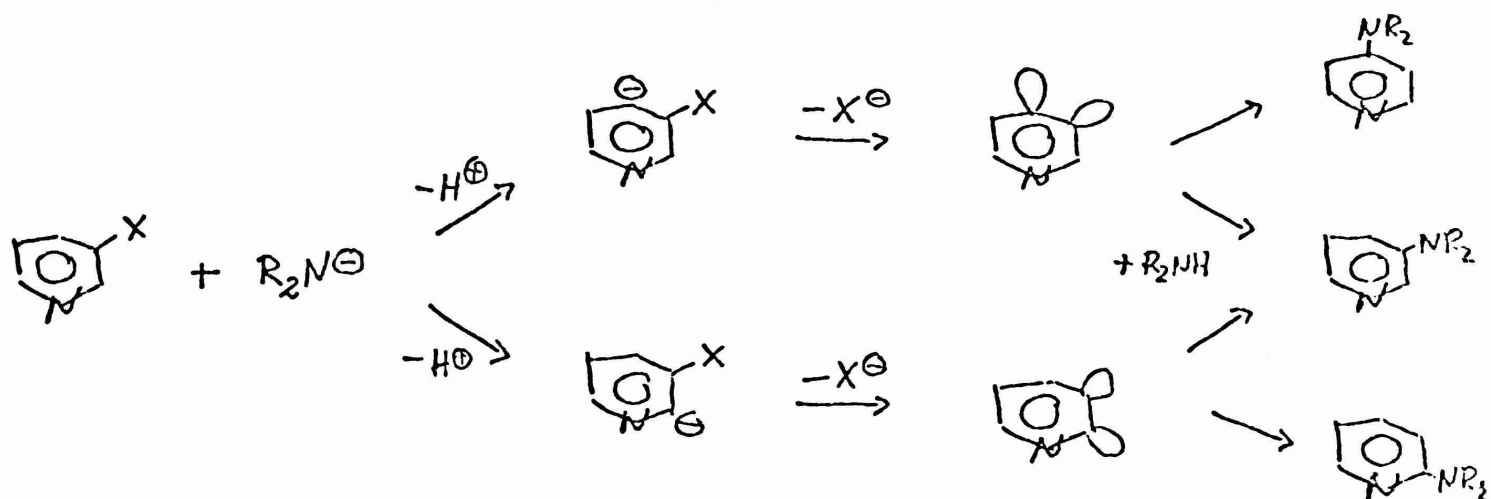
First of all, the formation of the 1, 2-hetaryne necessitates the removal of a proton

by the amide ion to form a carbanion. Two carbanions are possible, the 2-pyridinyl

anion, and the 4-pyridinyl anion. We have calculated the relative stability of

these carbanions in the case where X is hydrogen. The results are shown in Table 6,

and indicate that the 4-carbanion is 0.08 eV (1.9 kcal) more stable than the

2-carbanion. Fortunately, recent experimental data confirms this stability ordering,

Table 6: Heteroaromatic Carbanions

Parent	Position	E_{total} (eV)	E(parent) – E (anion)
	2	-529.75	—
	3	-530.00	—
	4	-529.83	—
	2	-536.04	—
	3	-536.18	—
	4	-536.06	—
	3	-536.78	8.77
	4	-536.85	8.70
	2	-537.60	9.01
	4	-537.67	8.94
	5	-538.07	8.54
	2	-537.45	8.81

since base-catalyzed deuterium exchange studies on pyridine and 3-chloropyridine

indicate that exchange predominates at the 4-position over the 2-position in both

cases.[14] The carbanions subsequently eliminate halide ion to form the 1, 2-hetaryne. The combination of the preferred formation of the 4-carbanion, which is the precursor of the 3,4-didehydropyridine, together with the greater stability (0.83 eV or 19 kcal/mole, Table 3) of this hetaryne over the 2,3-didehydropyridine, accounts for the facts. It is worth reiterating that the predominant factor against the 2,3-hetaryne is the nitrogen lone pair destabilization of the radical lobes.

In this context, on 'removal' of the nitrogen lone pair by protonation[14], alkylation[15], or N-oxide formation[15,16], deuterium exchange takes place preferentially at the 2-position, through the respective 2-pyridinyl carbanions. Again these experimental results are in harmony with EHT calculations, since the results of Table 6 indicate comparable stability for the 2- and 4- carbanions once the nitrogen lone pair has been protonated.

Although little information is available on the 1,2-didehydro intermediates derived from the diazines, some excellent experimental work has recently been reported on base-catalyzed deuterium exchange in these molecules.[17] The half-lives (in minutes) obtained for the exchange, using 0.23M sodium methoxide in O-deuteromethanol at 165° C are
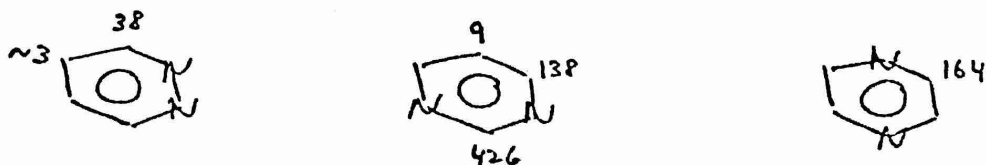
Inspection of Table 6 shows again that within each diazine the relative order of exchange half-lives is correctly predicted by the carbanion stabilities. The

comparison of the total energies of carbanions from different diazines cannot be made, since the total energies are dominated by the relative disposition of the nitrogens. To obtain a crude estimate of such a stability sequence the anion energies are subtracted from the parent energies in Table 6. This gives the energy ordering
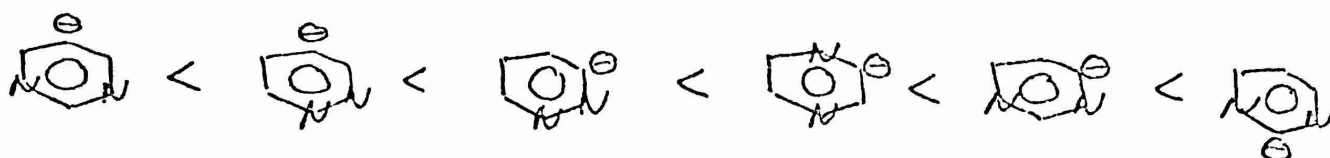
Although the general trend is reproduced, our calculations reverse the sequence for the 4-pyridazinyl anion and 5-pyrimidinyl anion(but the experimental value for the former is only approximate), and for the 4-pyrimidinyl anion and 2-pyrazinyl anion (where the experimental half-lives are very close). Considering the neglect of solvent effects, and the possibility of competitive exchange mechanisms, a perfect agreement is unlikely.

Some experimental data is available on the orientation effects in the addition of nucleophiles to the 1,2-dehydro intermediates. Whereas only one final product is possible from 1,2-didehydrobenzene, 3,4-didehydropyridine could undergo nucleophilic attack at the 3- or 4-positions to give different product. The addition of ammonia or piperidine to 3,4-didehydropyridine indicates a preference for nucleophilic addition at the 4-position.[3-5] Previously we have shown that EHT electron densities and total energies of the reaction intermediates successfully correlate orientation effects in nucleophilic substitution.[18] The total electron densities of Table 3 suggest that for 3,4-didehydropyridine preferential nucleophilic attack

should occur at the 4-position, as a consequence of its lower total electron density (3.97 against 4.35 electrons). In addition, the total energies of the pyridinyl anions confirm this preference. Localizing a hydride ion, chosen as a model for the amine nucleophile, at the 3- or 4- radical lobes of 3,4-didehydropyridine produces respectively the 4- or 3-pyridinyl anion. Since the 3-pyridinyl anion is 0.17 eV more stable than the 4-isomer (Table 2) nucleophilic attack should be preferred at the 4-position. As we have indicated[18], when both orientation criteria lead to the same conclusion, we can be confident that they provide a reasonable account of the observed effects. In this case, the preferred nucleophilic attack occurs at the 4-position. Although no experimental data has been published, our calculations indicate that the 3,4-didehydro intermediate derived from the pyridinium ion should undergo preferential nucleophilic addition at the 4-position also. In 3,4-didehydroquinoline the preferred addition takes place again at the 4-position, which is also reproduced by our calculations.[19]

Of some interest is the exclusive formation of 4-substituted products in the reaction of 5-bromopyrimidine with piperidine.[20] This suggests that the 4,5-didehydropyrimidine intermediate undergoes preferential nucleophilic attack at the 4-, rather than the 5-position. Again, total electron densities and the total energies of the pyrimidinyl anions are both in agreement with this orientational effect. On the basis of this experimental result, it can be seriously questioned whether the 2,3-didehydropyridine is not formed during the dehydrohalogenation of 2-halopyridines.[21] As a result of this reaction, the 2-substituted product is formed exclusively, and it was therefore argued that 2,3-didehydropyridine would have led

to the formation of some 3-substituted product. In fact, it was concluded that if the 2,3-hetaryne intervenes, the 3-isomer should be the predominant product, as a consequence of the electron withdrawal by nitrogen. Objections have been raised to this interpretation, since a strong orientation effect, similar to that found in 4,5-didehydropyrimidine, may be operative.[22] Our calculations provide evidence in favor of this objection. Both total electron densities and total energies of the pyridinyl anions predict preferential nucleophilic attack at the 2-position, rather than the 3-position. On the basis of our calculations, deprotonation of pyridine at the 3-position is energetically favored over the 2- and 4-positions. This renders it rather likely that the 2,3-didehydropyridine may indeed be the intermediate in this reaction, and a more detailed experimental study of this point seems advisable.

In the dehydrohalogenation of 4-halopyridazine, two 1,2-didehydro intermediates could be formed, the 3,4- and 4,5- didehydropyridazines. Our calculations indicate that the 4,5-isomer should be more stable, again due to the dominant effect of the lone pair destabilization. Because of the symmetry of the 4,5-isomer, no orientation effects are possible. In the unsymmetric 3,4-isomer, nucleophilic attack could lead to either a 3- or a 4- substitutes product. However, the differences in the total electron densities and in the anion energies are exceedingly small, and predict opposite orientations. This suggests that very little, if any, orientation effect is expected for the intermediates from 4-halopyridazine. Unfortunately, no experimental data is available.

The lack of experimental data on the 1,3-and 1,4-didehydroaromatics prevent us from confirming some of the interesting conclusions reached in these

calculations.[23] However, there has been some speculation on the 2,6-didehydro-pyridine as a reaction intermediate.[6] Again, Hückel molecular orbital calculations predict this 1,3-dehydro system to be stabilized by conjugation with the nitrogen lone pair. In our EHT calculations, and the attendant theoretical analysis, the 2,6-isomer clearly emerges as the least stable of the six possible hetarynes formed from pyridine (A-F). Once again, we attribute this finding to destabilization by the nitrogen lone pair, since even the 3,5-isomer (E) in which the lone pair is furthest from the radical lobes is energetically favored by 0.84 eV over the 2,6-isomer. This provides an explanation of the failure of all reported attempts to generate this species.[24]

The effect of the nitrogen lone pair is also revealed in an interesting way in the 1,3-overlap populations. Except in those instances where the lone pair is flanked by the radical lobes, the 1,3-overlap populations are all small but positive, and close to that of 1,3-benzyne. In 2,6-didehydropyridine, 2,4-didehydropyrimidine, and 2,6-didehydropyrazine, where the nitrogen flanks the radical lobes, the overlap populations are still small, but more significantly of negative sign. Clearly the nitrogen lone pair inhibits a direct bonding interaction of the 1,3-radical lobes. It is interesting to find that protonation of the nitrogen lone pair in 2,6-didehydropyridine again results in a slightly positive 1,3-overlap population, there-fore restoring the direct, through-space interaction found in 1,3-didehydrobenzene.

Recently we have noted a preliminary account of semiempirical SCF calcula-tions on the hetarynes by Yonezawa, Konishi, and Kato,[25] which we would like to to bring to the reader's attention. These calculations are able to decide if the ground state of the molecule is in fact a singlet, something which our calculations are not able to do.

ACKNOWLEDGEMENT

R E F E R E N C E S

1. Cornell University.

2. The Puerto Rico Nuclear Center is operated by the University of Puerto Rico for the U.S. Atomic Energy Commission under contract No. AT (40-1) 1833.

3. H. J. den Hertog and H. C. Van der Plas in "Advances in Heterocyclic Chemistry", A. R. Katritzky (Editor), Vol. 4, p. 121.

4. T. Kaufmann, Angew. Chem., 77, 557 (1965).

5. R. W. Hoffmann, "Dehydrobenzene and Cycloalkynes," Academic Press, New York, N. Y. (1967).

6. H. L. Jones and D. L. Beveridge, Tetrahedron Letters, 1577 (1964).

7. a) N. Y. Pieterse and H. J. den Hertog, Rec. Trav. Chim. 80, 1376 (1961)

   b) T. Kaufmann and F. B. Boettcher, Angew. Chem., 73, 65 (1961); Chem. Ber., 95, 1528 (1962).

8. H. J. den Hertog, M. J. Pieterse, and D. J. Buurman, Rec. Trav. Chim., 83, 1173 (1963).

9. R. Hoffmann, J. Chem. Phys., 39, 1397 (1963), and subsequent papers.

10. R. Hoffmann, A. Imamura, and W. J. Hehre, J. Am. Chem. Soc., 90, 1499 (1968).

11. The species 135 has three-fold symmetry, so that the wavefunctions fall into an (a) and (e) group classification. A basis can still be chosen for the degenerate representations which is consistent with the lower symmetry of the two-fold axis.

12. F. A. Cotton, "Chemical Applications of Group Theory", Interscience Publishers, New York, N. Y. (1963), p. 163.

13. A similar ordering is observed for pyrazine in recently published ab initio calculations in a Gaussian basis: E. Clementi, J. Chem. Phys., 46, 4737 (1967), and J. D. Petke, J. L. Whitten, and J. A. Ryan, J. Chem. Phys., 48, 953 (1968).

14. J. A. Zoltewicz and C. L. Smith, J. Am. Chem. Soc., 88, 4766 (1966); 89, 3358 (1967).

15. R. Abramovitch, Chem. Comm., 55 (1967).

16. J. A. Zoltewicz and G. M. Kauffman, Tetrahedron Letters, 337 (1967).

17. J. A. Zoltewicz, Abstracts of 155th ACS Meeting, San Francisco, April, 1968.

18. W. Adam and A. Grimison, Tetrahedron, 21, 3417 (1965).

19. a) W. Adam, A. Grimison, and R. Hoffmann, unpublished results.

    b) T. Kauffmann, F. P. Boettcher, and J. Hansen, Ann., 659, 102 (1962).

20. T. Kauffmann, J. Hansen, K. Udluft, and R. Wirthwein, Angew. Chem., 76, 590 (1964).

21. R. Wirthwein, Ph. D. Thesis, Darmstadt Institute of Technology, 1966.

22. Reference 1, page 133.

23. R. S. Berry, J. Clardy, and M. E. Schafer, Tetrahedron Letters, 1003, 1011 (1965)

24. Reference 2, page 571; reference 3, p. 311.

25. T. Yonezawa, H. Konishi and H. Kato, Bull. Chem. Soc. Jap., 41, 1031 (1968).